Thesis for the Degree of Licentiate of Engineering

Spectroscopic Studies of Low Temperature Polymer Electrolyte Membrane Fuel Cells

Mikael Holber

CHALMERS

Department of Applied Physics
Chalmers University of Technology
Göteborg, 2014

Spectroscopic Studies of Low Temperature Polymer Electrolyte Membrane Fuel Cells

Mikael Holber

Göteborg, 2014

Department of Applied Physics
Chalmers University of Technology
SE-412 96 Göteborg, Sweden
Telephone +46 (0)31-772 1000

Chalmers Reproservice
Göteborg, Sweden 2014

Spectroscopic Studies of Low Temperature Polymer Electrolyte Membrane Fuel Cells

Mikael Holber
Department of Applied Physics
Chalmers University of Technology

Abstract

Fuel cell technology is one of the many competing technologies in the future of energy conversion and transport. With a growing demand for efficient, versatile and environmental friendly alternatives to the internal combustion engine, fuel cells show promising potential where batteries and grid-electricity are not available.

For portable and transport applications, the low temperature Polymer Electrolyte Membrane Fuel Cell (PEMFC) is the most promising candidate. With a simple design, high power density and fast start-up, this technology have advanced quickly during the last decade with numerous field trials of several big automotive companies. However, two important challenges still remain.

The current PEMFC system is still several times more expensive than competing technologies, even in serial production. Alternative cheaper materials, as well as improved design and manufacturing techniques can ultimately lower the cost.

The durability of the PEMFC system must also be improved to compete with current technologies. The US Department of Energy estimates that the durability of a fuel cell stack need to reach no less than 5000 operating hours to be a competitive option. In the fuel cell stack, the membrane electrode assembly is known to be the limiting factor in durability tests.

In this thesis, Raman spectroscopy and X-ray Photoelectron Spectroscopy (XPS) are used to detect and identify degradation mechanisms in membranes and electrodes used in PEMFC. The two main degradation mechanisms detected in poly-fluorosulfonic acid-based (PFSA) membranes are loss of active end groups and degradation of the polymer backbone (cutting of the polymer chain). Both these mechanisms are quantified by Raman spectroscopy. Degradation of the backbone, and carbon migration from the electrodes into the membrane are certain signs of an upcoming failure of the membrane, this degradation is measured in detail with micro-Raman spectroscopy. Finally, XPS is used to measure the oxidation state and particle distribution in the interface between the electrodes and the membrane. A lowered concentration of active catalyst in electrodes lowers the efficiency of the fuel cell and leads to rapid degradation.

Keywords: fuel cell, PEMFC, degradation, PFSA, Raman, XPS, Nafion

List of Publications

This thesis is based on the work presented in the following papers:

I **Raman Investigation of Degradation and Ageing Effects in Fuel Cell Membranes**
M. Holber, A. Carlsson, P. Jacobsson, L. Jörissen, and P. Johansson, *ECS Transactions, 25 (1), 2009, pp. 807-811.*

II **Raman Spectroscopy of an Aged Low Temperature Polymer Electrolyte Fuel Cell Membrane**
M. Holber, P. Johansson, and P. Jacobsson, *Fuel Cells, 3, 2011, pp. 459-464.*

III **Spectroscopic Detection of Local Platinum Degradation in Polymer Electrolyte Membrane Fuel Cells**
M. Holber, A. Haug, M. Schulze, A. Selimovic, S. Escribano, L. Guetaz, L. Merlo, K. A. Friedrich, P. Jacobsson, and P. Johansson, *submitted.*

Contribution Report

My contributions to the papers included in this thesis:

I Prepared and performed all Raman spectroscopy experiments, participated in analyzing and concluding the data. Wrote the first draft and main author of the paper.

II Contributed with performing all experiments. Analyzed the data and participated in conclusions. Wrote the first draft and handled integration of comments from co-authors. Main author of the paper.

III Planned and performed Raman spectroscopy and X-ray Photo-electron Spectroscopy experiments. Participated in the analysis and conclusion of results. Wrote the first draft and main author of the paper.

Glossary

Term	Description	Definition
Electro-osmotic drag	Mechanism of water movement in electric fields	page 14
Back diffusion	Water diffusion towards a dry anode	page 14
Oswald ripening	Particle growth via dissolution and redeposition	page 20
Coalescence	Process where smaller particles join into large ones	page 20
Post-mortem analysis	Analysis after failure of cell or material	page 22

List of Abbreviations

Abbreviation	Description	Definition
ICE	Internal combustion engine	page 3
CNG	Compressed natural gas	page 4
HEV	Hybrid electric vehicle	page 5
PEMFC	Polymer electrolyte membrane fuel cell	page 8
HOR	Hydrogen oxidation reaction	page 8
ORR	Oxygen reduction reaction	page 8
BPP	Bipolar plate	page 9
GDL	Gas diffusion layer	page 9
PEM	Polymer electrolyte membrane	page 9
AL	Active layer	page 9
MPL	Micro porous layer	page 10
Pt	Platinum	page 11
LSC	Long side chain	page 11
SSC	Short side chain	page 11
MEA	Membrane electrode assembly	page 11
PFSA	Poly-fluorosulfonic acid-based polymer	page 12
OCV	Open circuit voltage	page 15
OCP	Open circuit potential	page 20
Ru	Ruthenium	page 22
PTFE	Polytetrafluoroethylene	page 22
EIS	Electrochemical impedance spectroscopy	page 27
XPS	X-ray photo-electron spectroscopy	page 29
SEM	Scanning electron microscopy	page 29
TEM	Transmission electron microscopy	page 29
STEM	Scanning transmission electron microscopy	page 29
EDX	Energy dispersive X-ray spectroscopy	page 30
EELS	Electron energy loss spectroscopy	page 30

Contents

Chapter 1

Energy

Energy is literally what makes the world revolve. With enough energy mankind can overcome most of our global challenges; pure water can be produced from thin air or salty ocean water, with this water we could produce enough food for a growing population [1, 2]. Looking at the energy consumption today we see some interesting facts; even as OECD countries like Sweden reduce our energy consumption per capita, the total energy consumption of the world increases [3]. On top of this, with environmental threats such as global warming the outcast for success is not the brightest. However, recent advances in renewable energy technology and public awareness of the environmental issues at hand give "new fuel" to both research and industry.

The energy sources used today are a mix of three types; nuclear, fossil, and renewables. These three types of energy sources provide all energy we use on a daily basis. Nuclear and fossil energy are non-renewable sources which are finite and impact the environment through pollution and other hazards to mankind. The third option, renewable energy, comes in different forms from solid biomass from the forest to gaseous biogas produced from organic waste. This family of energy sources will be the sustainable alternative in the future. The main debate now is how close to that future we are?

Renewable sources of energy are those that can be renewed during our lifetime. Examples are geothermal heat, solar-, wind-, wave-power etc. where the energy cannot be stored in its original form [4]. Other renewable sources can be stored, e.g. biomass (solid) and biofuel (liquid), with high energy content. Renewable energy sources have many advantages compared to fossil and nuclear but also some disadvantages such as high price and low energy content. Competition with food production makes the use of these fuels, in some cases, politically challenging [5, 6].

1.1 Oil as an Economy

Oil as an economy refers to that the price of oil governs many other prices. For example, if the price of oil increases because of conflicts or war, the price of fresh fruit in Sweden may also increase due to higher transportation costs. The energy situation in Europe and the rest of the world is largely dependent on the availability of oil due to our dependence

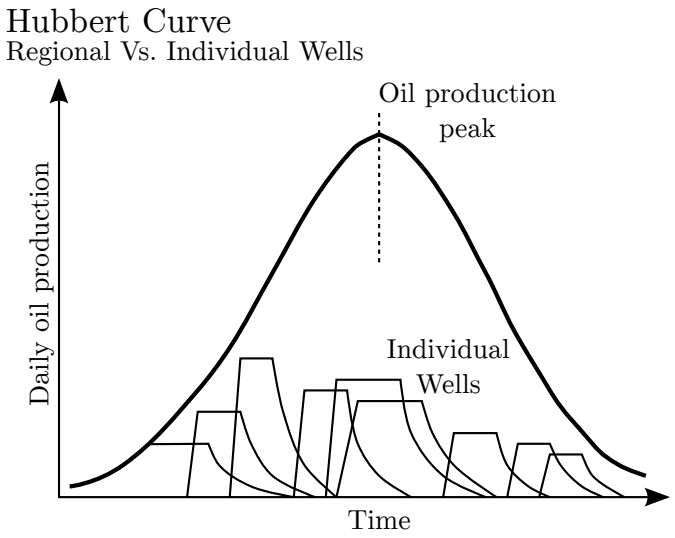

Figure 1.1: The Hubbert curve describe the global relationship between individual oil wells and the total production of oil. A decline in discoveries of new oil wells would be the first indicator of a peak in oil production or "peak oil" according to the Hubbert curve [7].

of energy for both transportation and stationary applications.

During the 20^{th} Century we have made ourselves more and more dependent on oil. Oil is refined into polymers, gasoline, diesel and other lighter hydrocarbons. These are also used to synthesize other compounds such as ethanol and methanol. The primary reason for our fixation to oil is that historically the price and availability have been excellent. This might, however, be on the verge of changing; peak oil and global warming have shed a new light on our consumption of non-renewable energy.

Global warming has during recent years been accepted by the majority of the scientific community to be a fact caused by the excessive use of fossil fuels resulting in an increase of carbon dioxide in the atmosphere. The idea to use renewable fuel instead of fossil fuels is not to decrease the usage of the total amount of fuel, but to use energy where the carbon dioxide can be recycled within 1-100 years.

Peak oil is the term describing the problem of energy resource depletion and was described by the geologist M. King Hubbert in 1956 [7], see figure 1.1. Peak oil could have a negative effect on the economic system which in many aspects are based on cheap readily available energy, the dominating of which is oil responsible for 41% of the total fuel consumption and 95% of the fuel consumption in the transport sector globally [8]. There are ongoing discussions whether we have already passed peak oil or not [9, 10, 11, 12].

1.2 Fossil Fuels

Fossil fuels originate from natural anaerobic decomposition of organisms buried under ground or in water reservoirs. The fossil remains have been chemically changed due to high pressure and heat during a long period of time, sometimes exceeding 650 million years. Due to the organic origin of the fuel a high carbon content is the common denominator for all the fuels whether solid, liquid or gaseous at ambient pressure and temperature.

Fossil fuels have been the dominating energy source for the transport industry since the introduction of the internal combustion engine (ICE). Other alternatives such as electrical vehicles were popular during the beginning of the 20^{th} Century, but were marginalized due to the low price of gasoline.

1.3 Renewable Energy

The term "Renewable energy" implies energy that can be renewed within our life time. The amount of renewable energy used globally has, during the last 25 years, been constant around 10% of the total global energy supply with the larger part being grid power production [13]. The smaller part of fuels are often referred to as biofuels and used as energy carriers; examples are bioethanol, biomethanol and biogas.

Many renewable energy sources have been part of our society for thousands of years; from heating homes with wood fires to producing flour from grain using windmills and water mills. These techniques are simple and reliable but they are not very energy efficient or power dense. There are also variations in the production as the sun goes down (solar power), the wind stops blowing (wind power) or during dry periods (hydro power). The solution is to either create a continuous and controlled production or an efficient energy storage. One way to store energy is chemically as hydrogen gas.

1.4 Hydrogen

One common misconception with fuels is that they are not a source of energy but energy carriers. Fossil fuels are for example located in oil and gas findings, pumped to the surface and refined to various energy carriers. These reservoirs were created during millions of years and stored until the industrialization of mankind. Hydrogen is not a fuel that can be found in abundance anywhere, but hydrogen can be produced through various different processes with a high efficiency and very few by-products. Most energy sources and carriers can be converted into hydrogen and many chemical plants have very pure hydrogen as a waste product from other chemical processes.

1.4.1 Production

Hydrogen production can be divided in three main categories; reformation of hydrocarbons, which can be made from fossil or biomass fuel, electrolysis of water, which basically acts as a reverse fuel cell, and photo catalytic water splitting into hydrogen. Reformation is today the technique that generates the most hydrogen, and steam reforming of natural gas alone generate 50% of the world's supply of hydrogen and fossil fuels account for 96% of the total production [14, 15]. Hydrogen produced with this technique generates carbon dioxide and depending on the fuel source, this could add to global warming. This technique is on the other hand an important step towards fuel cells in transportation as the reformation process can be done on-board the vehicles and therefore use the current infrastructure for gasoline for example.

	Hydrogen	Gasoline vapor	Natural gas
Flammability limits (in air)	4 - 74%	1.4 - 7.6%	5.3 - 15%
Explosion limits (in air)	18.3 - 59.0%	1.1 - 3.3%	5.7 - 14%
Ignition Energy (mJ)	0.02	0.20	0.29
Flame temp. in air (°C)	2045	2197	1875
Stoichiometric mixture (most easily ignited in air)	29%	2%	9%

Table 1.1: Hydrogen requires a higher concentration in the air to ignite than both gasoline and natural gas, which in some aspects makes it equally or more safe than conventional fuels. Recreated from [17].

1.4.2 Storage

Hydrogen is the smallest molecule there is and can therefore escape through materials, this need to be kept in mind when designing storage vessels. Most metallic cylinders can contain hydrogen with a very low permeability rate, but polymers and composites can cause problems. This property can also be positive as in the event of evacuation of a cylinder, hydrogen will be evacuated and dispersed much faster than other heavier gases such as compressed natural gas (CNG [16]).

1.4.3 Safety

Safety is usually the primary concern when you discuss hydrogen as a fuel on-board a vehicle or in other consumer products. Many of us know about the Hindenburg accident in 1937 and though the reason of the initial ignition of the airship is not known the same type of disaster could have happened if the airship would have been filled with CNG. In fact, compared to conventional fuels hydrogen is not easier to ignite than for example gasoline vapor or natural gas, see table 1.1 [17]. Hydrogen is safely used on a daily basis in many different chemical processes and can be used and stored safely but as with all flammable fuels you need to consider the safety aspects.

1.4.4 The Hydrogen Society

For an energy system to be sustainable one must take all steps; production, distribution, storage, conversion and finally environmental and health impacts into account. Hydrogen could very well be the energy carrier that dominates transportation in the future, however, for this to become a reality the system needs to be efficient and economically competitive.

Chapter 2

The Fuel Cell

While finding new and improving already established renewable sources of energy is important, the energy conversion also has to be improved. In the automotive sector, the recent paradigm shift is the hybridization of the traditional ICE with an electric engine, creating hybrid electric vehicles of various kinds (HEV). This is a very important step towards true EVs using only electricity from the grid, stored in batteries, as fuel. The alternative route to pure electric cars is to store the energy chemically in the same manner as done today with natural gas, diesel, gasoline and other liquid and gaseous fuels, and convert it to electric energy. In this chapter we look into all the components of fuel cells, their purpose, their limitations, and what is important when designing fuel cell materials.

2.1 Basics and History

A fuel cell is a device converting electric energy from chemically stored energy without combustion. The fuel cell consists of an anode and a cathode, where the chemical reactions take place, and an electrolyte for proton transport (see figure 2.1). Fuel cells are considered a modern technology, but the first fuel cell was invented by William Grove already in 1839 [16]. One large step for the technology was in 1965 when the space shuttle Gemini 5 used fuel cells to power its electronic equipment. Fuel cells were again used for the Apollo space program to produce electricity, heating and fresh drinking water. In line with this work, PowerCell AB has developed and demonstrated a compact fuel cell system using diesel as fuel [18, 19]. Many types of fuel cells exist, see table 2.1.

2.2 Efficiency

The direct conversion of chemical energy to electrical energy offer an improved efficiency compared to an ICE. For the ICE, the exothermic reaction of the combustion release energy in the forms of heat, which is translated into work according to the first law of thermodynamics. The theoretical efficiency ν_{theory} is defined as:

$$\nu_{theory} = \frac{T_2 - T_1}{T_2} \tag{2.1}$$

	PEMFC	DMFC	PAFC	AFC	MCFC	SOFC
Electrolyte	Fluorinated/ Organic polymer	Fluorinated/ Organic polymer	H_3PO_4 (aq)	KOH (aq)	Molten carbonate	Yttria-Zirconia
Temp. range (°C)	80-100	80-100	170-220	25-220	600-100	600-1000
Fuel	H_2	Methanol	H_2	H_2	H_2 and CH_4	H_2, CH_4 and CO
Charge carrier	H^+	H^+	H^+	OH^-	CO_3^{2-}	O^{2-}
Catalyst	Pt	Pt	Pt	Pt	Ni	Ni
Power range (kW)	0.001-1000	0.001-100	10-100	1-100	100-100000	10-100000
Advantages	High power density, fast start-up and shut down, operates at low temperatures	High power density, fast start-up and shut down, operates at low temperatures, simple storage of fuel	High fuel efficiency when combined with heat and power, low sensitivity to impurities	Can be combined with heat and power	High fuel efficiency when combined with heat and power, low sensitivity to impurities	High fuel efficiency when combined with heat and power, low sensitivity to impurities
Disadvantages	Sensitive to impurities and CO, expensive catalyst	Short life-time, poisonous fuel, fast degradation, low power density	Long start-up time, low power density	Sensitive to CO_2 poisoning making purification expensive, electrolyte managment	Expensive materials, poor durability, high temperature corrosion and breakdown of components	Slow start-up, high temperature corrosion and breakdown of components, require significant thermal shielding

Table 2.1: The most important properties, advantages and disadvantages of the different fuel cell technologies.

Where T_2 is the upper temperature limit and T_1 is the lower temperature limit of the reaction. The efficiency of the combustion is also limited by the Carnot cycle:

$$Q_{Carnot} = \frac{T_1}{T_2} Q_{react} \tag{2.2}$$

The maximum theoretical efficiency of according to the Carnot cycle is about 50% [16]. A total system efficiency of 40% for an ICE is considered a very efficient system, and at idling only a few percent is not unusual. Fuel cells on the other hand, are not limited by the Carnot cycle. The electrochemical mechanism convert the chemical energy into electrical energy directly and only a portion of the energy is lost as latent heat of reaction, Q_{lat}. The theoretical efficiency is:

$$\nu_{theory} = \frac{Q_{react} - Q_{lat}}{Q_{react}} \tag{2.3}$$

For a fuel cell with hydrogen as the fuel the maximum efficiency is 83% [16]. As with most systems there are losses and for the fuel cell these are mainly related to activation losses, internal resistance and mass transport limitations at high loads. A fuel cell system above 50% efficiency is considered to be feasible to manufacture with state-of-the-art materials and designs available.

2.3 Fuels

As mentioned in the previous section, the primary fuel of the low temperature fuel cells is hydrogen. It is, however, possible to combine the fuel cell with a fuel converter from other fuels. An example is the diesel reformer which converts diesel into a hydrogen rich gas through a steam reforming process involving high temperature and steam as shown in equation 2.4.

$$CH_4 + H_2O \overset{+\Delta}{\rightleftarrows} CO + 3H_2 \tag{2.4}$$

The process, however, produces large amounts of carbon monoxide prone to poison the catalyst in low temperature fuel cells. The carbon monoxide can be reduced by a gas-shift reaction (equation 2.5) at low temperature yielding additional hydrogen gas. A diesel reformer yields approximately 45% hydrogen; the rest being nitrogen, carbon dioxide and traces of carbon monoxide and hydrocarbons.

$$CO + H_2O \rightarrow CO_2 + H_2 \tag{2.5}$$

The steam reforming reaction is strongly endothermic, while the gas-shift reaction is mildly exothermic. The whole process requires energy both during start-up/warm-up and under steady-state operation. This can be achieved by recycling unused fuel from the fuel cell into a catalytic burner heating the reformer.

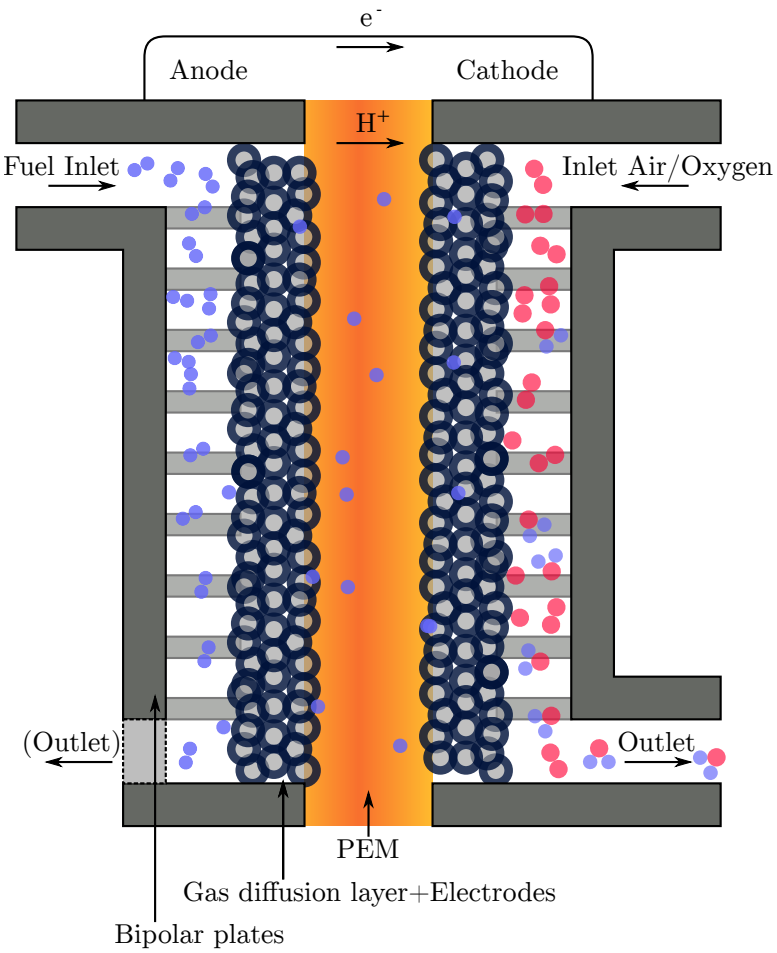

Figure 2.1: Schematic of a PEMFC. Fuel containing hydrogen is feed to the anode and oxygen (often air) is feed to the cathode, the reaction occurs when a load is placed between the current collector plates and the waste product is pure water. If pure hydrogen is used, it is not necessary to have an anode outlet as all gas is consumed.

2.4 The Polymer Electrolyte Membrane Fuel Cell (PEMFC)

The focus of this work is on polymer electrolyte membrane fuel cells (PEMFC). The fuel for PEMFC is hydrogen gas and as the schematic in figure 2.1 shows, the hydrogen gas is fed into the anode side of a fuel cell membrane and oxygen is fed into the fuel cell on the other side. The electrodes on both anode and cathode side of the membrane contain an electro-catalyst which split the hydrogen gas on the anode electrode into protons, this reaction is referred to as the hydrogen oxidation reaction (HOR, equation 2.6). The protons are transported through the electrolyte membrane and recombined with electrons and oxygen ions at the cathode electrode to produce the only waste product; water. The cathode reaction is called oxygen reduction reaction (ORR, equation 2.7). The electrons are not conducted through the membrane, but through an external circuit to produce electricity.

$$2H_2 \rightarrow 4H^+ + 4e^- \tag{2.6}$$

$$4H^+ + 4e^- + O_2 \rightarrow 2H_2O \tag{2.7}$$

The PEMFC can be made into any shape and size to suit the application in terms of power required and space available. PEMFC has great potential in transport application mainly

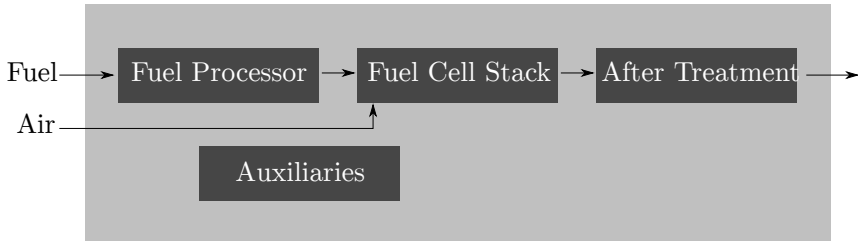

Figure 2.2: Schematics of a fuel cell system. Depending on application, fuel processor and after treatment are optional.

due to the high power density (around 1 W/cm^2) and the low temperature (80-120°C) which yields small, light stacks with fast start-up and easy thermal control. On the other hand, the main drawbacks are the high purity of the fuel required, expensive catalysts needed for the low-temperature reactions and poor durability under cycling conditions. A comparison of the different fuel cell technologies, their advantages and disadvantages, is made in table 2.1. In a fuel cell hybrid electric vehicle (FCHEV), the ICE is replaced by a highly efficient electric engine driven by a low noise fuel cell that can with a reformer be powered by a variety of different fuels. The total efficiency from tank-to-wheel can be higher than the ICE over a wide range of power outputs [20].

2.5 PEMFC Components

A PEMFC system can be split into four major components; fuel processor, fuel cell stack, after treatment and auxiliaries (see figure 2.2). This work focus on the fuel cell stack and how to increase its durability. When assembling a fuel cell stack, each cell in practice has an operation voltage of about 0.7 V. As the cells are connected in series the total voltage of the stack are the sum of all the cell voltages. For automotive industry, the stack voltage range typically from 40-200 V depending on application (auxiliary, range extender or primary source). The total current scales with the total area of the cell. For a very small fuel cell stack, air cooling can be sufficient to remove the excess heat. But for most fuel cells, a cooling water circuit is needed to remove the heat from each fuel cell unit.

The stack, in turn, also consists of four specific components, see figure 2.1. The basic components counting from the gas inlet are; bipolar plates (BPP) sometimes referred to as the current collectors, the gas diffusion layer (GDL), the electrodes which is a mix of carbon black and catalyst, and the polymer electrolyte membrane (PEM). We will look at all of these components, what their tasks are, and how they are assembled in the fuel cell.

2.5.1 Bipolar Plates (BPP)

The BPP have several important tasks; distribute the reactant gases over the entire surface, provide heat transfer for the electrochemical reactions, conduct the electrons produced and consumed at the active layers (AL), and act the mechanical support for the stack. When assembling a fuel cell stack, the BPP acting as anode in one cell will be the cathode bipolar plate for the next cell in the stack. If active cooling is needed, this is often integrated in the BPP between the anode and the cathode side of the plate. Because of the required low electric resistance the choice of material is either metals or composites. Composite BPP have the advantage of being chemically stable in the fuel cell environment, have low resis-

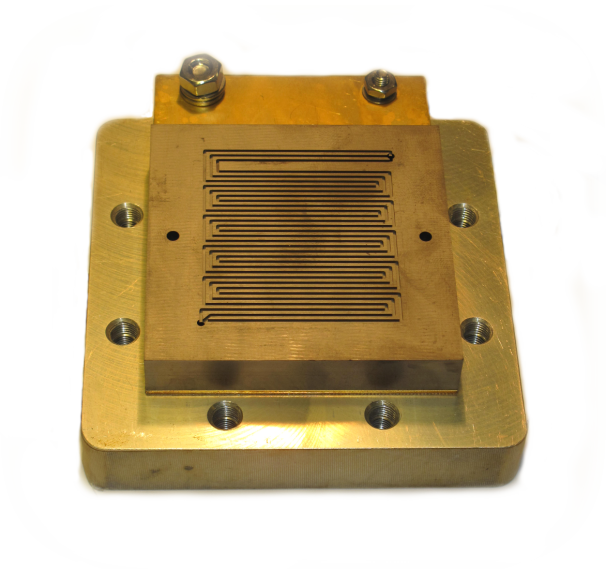

Figure 2.3: The experimental cell used for the aging experiments. The flow field has a "triple serpentine" pattern machined from a thick composite piece.

tance and being easy to machine. However, composite materials are often brittle, requiring thicker plates. This in turn leads to a larger total weight and size of the stack. Figure 2.3 shows the composite BPP used for this work. Metallic BPP on the other hand, are cheap and can be manufactured in micron thick plates, yielding thin stacks. The downside is that the conductivity often is lower than for composite plates and their chemical resistance is dependent on the metal alloy. Oxidation of metal BPP (rust) not only affects the mechanical stability and gas flow in the stack, but could also poison the catalyst and membrane. The BPP with active cooling is the single largest and heaviest component in the fuel cell and is responsible for at least 75% of the total weight of the stack.

An important aspect of the BPP is the flow field. The efficiency of the fuel cell is highly dependent on the how well the gas is distributed with the smallest pressure drop. The bipolar plates shown in figure 2.3 have a so called "triple serpentine" pattern. This ensures good distribution of gas balanced with three individual flow channels to lower the pressure drop.

2.5.2 Gas Diffusion Layer (GDL)

The GDL, usually a carbon based cloth or fiber network, is designed to have high gas permeability and good electric conductivity. The GDL is in direct contact with the BPP and electrodes with the task to evenly distribute the reactant gases and transport the electrons between them. A modern GDL has a hydrophobic coating to remove excess water and avoid flooding of the electrode surfaces (Figure 2.4). A typical GDL for PEMFC is constructed of woven layers of carbon fibers with a micrometer size diameter.

2.5.3 Electrodes

The electrodes, also known as the micro porous layer (MPL), the active layer (AL), or the catalyst layer, are composed of catalyst particles, carbon support, and a proton conducting matrix. The electrochemical catalyst is responsible for the fuel reaction in the fuel

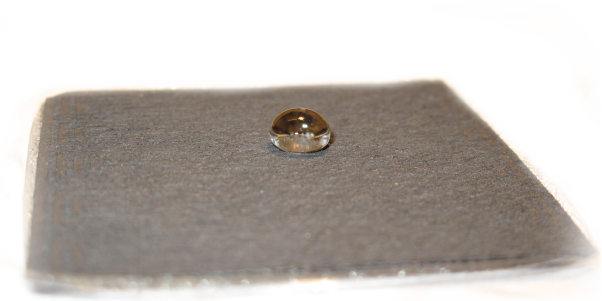

Figure 2.4: The GDL is treated with hydrophobic PFSA to improve the transport of excess product water away from the electrodes.

cell. The carbon support is the conductor between the catalyst and the GDL, leading the electron to and from the reaction sites. The proton conducting matrix is the glue which binds the reactants together and are also responsible for the proton transport between the reaction site and the PEM. Figure 2.5 depicts all parts and the 3D structure and relevant sizes. The porous structure yields easier gas transport and the proton-conducting matrix covering the support allows proton transport between the membrane and the reaction-site on the catalyst particles. The carbon support is used as electrical conduction between the BPP and the reaction sites, and the hydrophobic support aid the evaporation of product water produced at the reaction sites.

The catalyst for all low temperature fuel cells are platinum (Pt) based, and in the case of a system with a reformer, alloyed with ruthenium and cobalt to handle carbon monoxide. Platinum is the only known catalyst capable of splitting hydrogen into protons and electrons and recombining it with oxygen to form water. Therefore, platinum is present at both electrodes. The platinum catalyst is expensive and therefore it is important to have a low loading of catalyst. Research during the recent years have been successful and the loading for modern materials today is about 0.6 $\mu g/cm^2$ compared to 5 $\mu g/cm^2$ around year 2000 [21].

For PEM, three dominating polymer configurations compete today; long (LSC), intermediate, and short side chain (SSC) groups. Examples are Nafion®, 3M PFSA, and Aquivion [24]. The side chain groups' influence on ion conductivity, chemical resistance and mechanical strength is complex; shorter side chains will create smaller tubes and therefore lower ion conductivity and lower water uptake (swelling), but higher mechanical strength. Fewer ether links also give the polymer better chemical stability, but limits the polymers' flexibility.

For the performance of the fuel cell, it is crucial that the electrodes are as thin as possible. For this purpose the electrodes are deposited directly on the GDL or the PEM as a micrometer thick layer. Electrode manufacturing methods are printing, spraying, or brushing of an electrode ink containing a suspension of particles and carbon support. After being deposited on either GDL or membrane, the whole assembly is pressed together to form the membrane electrode assembly (MEA). This can be done before assembly of the fuel cell or

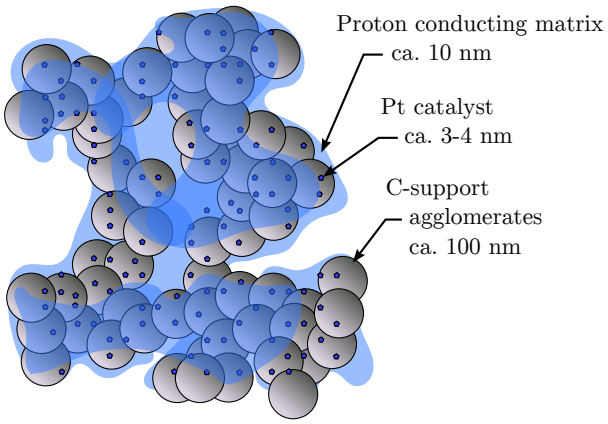

Figure 2.5: The structure of the catalyst layer is 3-dimensional and consists of a carbon based support (c-support) in the range of ∼100 *nm* with nano-meter sized Pt catalyst particles attached. To yield proton conductivity from the particles to the bulk membrane the structure is covered with a thin film of proton conducting matrix (often the same polymer as the membrane). The catalyst layer degradation can affect all three components, but by different mechanisms such as carbon corrosion, thinning of the proton conducting matrix, and loss of catalyst particles as shown in this picture. Inspired by Satish *et al* [22] and Zhang *et al* [23].

as a process by the heat and pressure at the first start-up.

2.5.4 Polymer Electrolyte Membrane (PEM)

The most important properties of the PEM are to:

- Facilitate proton transport from the anode to the cathode.
- Block gas crossover from one side to the other.
- Electrically insulate, to not short circuit the fuel cell.

These properties are fulfilled by poly-fluorosulfonic acid-based polymers (PFSA). In literature, the most commonly used PFSA is Nafion® developed by DuPont in the 1960's (figure 2.6) [25]. The fully fluorinated backbone gives the polymer a good chemical stability in the harsh environment present in the fuel cell.

Proton transport inside the PEM

PFSA-ionomers have hydrophobic backbone and hydrophilic end groups. The hydrophilic part can absorb large quantities of water, the weight of the material can be increased by up to 50% when fully hydrated [27]. The long polymer chains align and with the right length of the side chain groups this will create a stable structure of hydrophilic tubes with a hydrophobic matrix in between (figure 2.7) [28, 29], however, this model structure is debated [30, 31]. The proton transport is a product of these tubes, a close enough distance between the hydrophilic end groups and sufficient amount of water molecules in the tubes, allow the protons to "jump" from water molecule to water molecule creating H_3O^+ ions which move in the electric potential field created by the anode and cathode potentials. The ability to easily donate protons to water molecules creating these hydronium ions (H_3O^+) makes the PFSA-membrane a super-acid. A fully hydrated Nafion membrane contains up to 21 H_2O

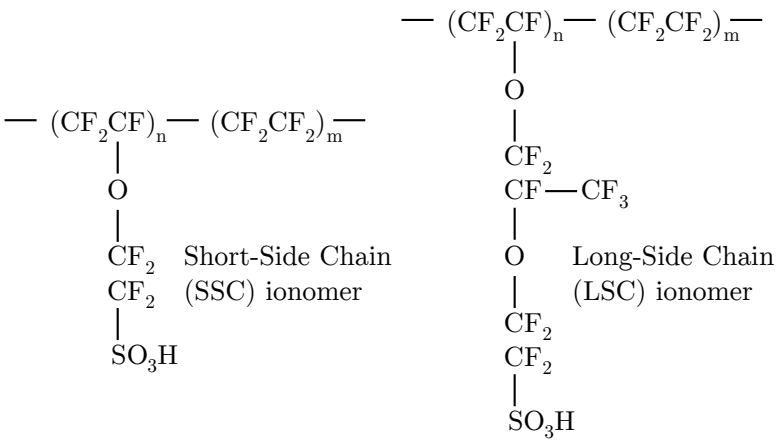

Figure 2.6: The chemical composition of long- and short-side chain ionomers used for fuel cell applications. This long-side chain ionomer is commercially known as Nafion® from DuPont and the short-side chain ionomer is produced by Solvay Solexis under the name of Aquivion® [26].

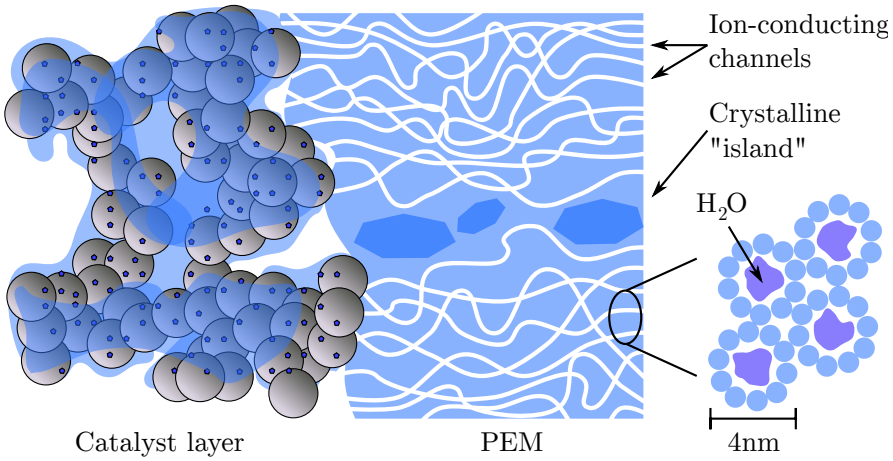

Figure 2.7: The structure of semi-crystalline ionomer on the nano-meter level is composed of ion-conducting channels linked together. The crystalline "islands" provide increased rigidity and stability to the polymer at elevated temperatures.

molecules per SO_3^--group, but this decreases if other cations are present in the membrane [32].

The internal resistance within the fuel cell is a sum of the electrical resistance and the proton transport in the PEM. The electrical resistance is usually very low as the electron transport takes place in graphite-like materials and stainless steel. The proton transport resistance in the membrane is usually magnitudes higher even though the protons are only transported through a very thin film. This is due to much larger mass of the proton and the limitation of ion transport in solid materials [33].

The thickness of today's membranes range from 20-150 μm depending on ionomer and manufacturing technique; the benefit with thinner membranes is higher ion conductivity and therefore a higher efficiency of the cell. Very thin membranes can on the other hand have a lowered performance due to cross over of gas and/or electrons between the anode and the cathode, which lowers the potential and the efficiency. A thinner membrane demands good mechanical stability to avoid pinhole-formation. Cross over of gases does not only

affect the performance, the chemical process taking place around the hole will release heat that further damages the membrane. Ultimately the fuel cell membrane breaks.

Water in the PEM

The humidification of the PEM is complex. Water can be supplied to the membrane in two ways: i) the ORR produces water, and ii) the incoming gases in the fuel cell can be humidified. It is common to supply 50-100% of humidity to the incoming gases of a PEMFC. On the other hand, water leaves the fuel cell with the excess gases. When it comes to water economy, water can be recycled and reused in the humidifiers.

A traditional PEM fuel cell operates between 60-95°C. In this temperature range it is easy to control the humidity keeping the PEM fully hydrated yielding a good performance. The main advantage with higher operation temperatures is the more efficient cooling system, making the total system efficiency higher. Also, the CO tolerance at higher temperatures improves, which simplifies the design for reformers in systems using hydrocarbons as fuels. However, at temperatures above 100°C, even with fully humidified gases, the membrane will have a low humidity, which requires a PEM with very high proton conductivity even at low humidities [34].

Inside the PEM water move in hydrophilic channels by several mechanisms. Electro-osmotic drag is when the hydronium ions (H_3O^+) are pulled by the electric field [27, 35], from the anode to the cathode. This can result in a flooding of the cathode and drying out of the anode. Each proton can pull a whole cluster of water molecules. This makes the electro-osmotic drag one of the dominating mechanisms in the PEM water balance. Back diffusion is when the water produced by the ORR at the cathode moves towards the anode. The water concentration is often lower on the anode side due to the electro-osmotic drag, but is counteracted somewhat by the back diffusion. Two other effects worth mentioning are thermal-osmotic drag and pressure driven hydraulic permeation. Usually these effects can be neglected, but may play a role for conditions of large thermal gradients or uneven back pressures.

The losses in the PEMFC

All interacting processes in a PEMFC make it a complex task to optimize the system efficiency. First the losses are outlined, dependent on operation voltage (figure 2.8). The polarization curve can be divided into three regions with low, medium and high current densities;

i) In the low current density region, fuel is abundant on both the anode and the cathode, the high concentration of fuel and the low consumption will allow the fuels to diffuse into the membrane (crossover) and react directly on the opposite electrode, this creates a chemical short circuit. Activation losses are associated to the speed of the electron-transfer on the catalyst. The ORR is several orders of magnitude slower than for the anode reaction.

ii) The dominant loss in the medium current density region is the ohmic resistance. The main resistance source is the proton transport.

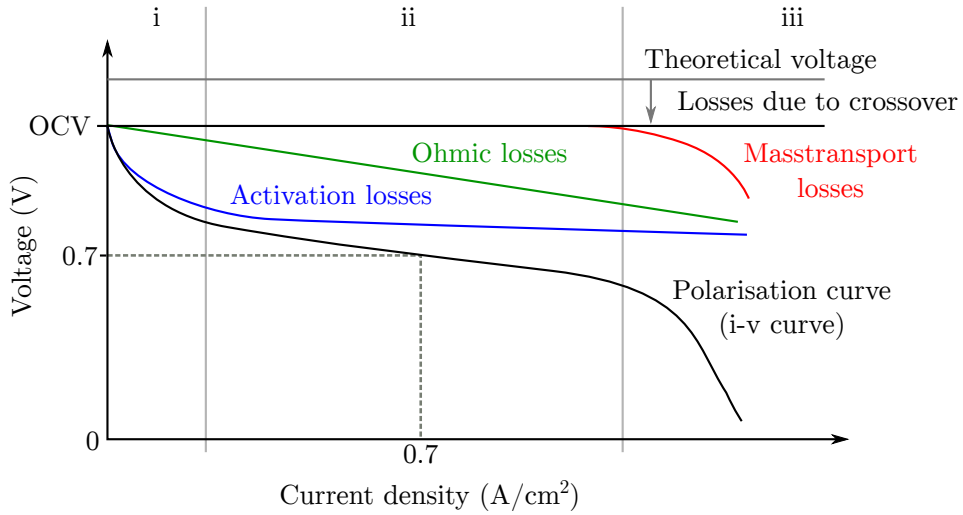

Figure 2.8: A summary of the voltage losses in the polarization curve. Inspired by Yousfi-Steiner *et al* [36].

iii) At high current densities, mass transport to the electrodes becomes the major loss. Narrow pores and droplet formation on the catalyst creates the state of fuel starvation, which can be mitigated with improved gas flow design.

Manufacturing of PEM

There are various methods to manufacture the PEM. Mechanical strength and orientation of polymer chains is highly dependent on parameters such as additives and processing temperature. With extrusion and casting there are possibilities to create gradients with reinforcements in the membrane [37]. The manufacturing parameters and additives used are often commercial secrets of the manufacturers. One example is radical scavengers, designed to increase the chemical stability of the membrane by reacting with the radicals produced under non-optimal working conditions such as open circuit voltage (OCV) [38].

2.6 Obstacles to PEMFC Commercialization

The ICE has had over 100 years of commercial use to improve and become the leading power converter in transportation and many other applications. For PEMFC to be a competitive option, it has to produce the same amount of energy, have similar dynamic properties (changing power quickly on demand), have a competitive cost, and a comparable life-time.

2.6.1 Material Cost

For some time, the significant cost for PEMFC has been the Pt-catalyst. The electrodes with the Pt-catalyst accounts for ca 50% of the total stack cost [39]. However, as catalyst loading has decreased, the focus on other components such as the sealings, GDL, BPP, and PEM has increased. Sealings in the fuel cell stack play an unexpected role. The temperature, pressure, hydrogen permeability, and chemical environment limit the choice of materials to highly specialized polymers. Reports from the US DOE show 10.8% of the total stack cost to come from the sealings, more than the PEM itself costs (8.4%) [39]. The corrosive resistant stainless steel in the BPP is expensive and has poor thermal properties,

however, with good design including cooling pockets, the BPP can be made very thin, and contribute to lighter stacks and higher power densities. The GDL is manufactured from inexpensive materials and the cost is already low.

2.6.2 Life-Length

With a large investment cost, being about 40% of the total system cost, the life-length of the stack must be comparable with already present technologies. An estimation of a life-time exceeding 5000 operating hours is needed for commercialization, somewhat dependent on market and application. Life-time experiments today range from 1000-26000 operating hours [37, 40, 41, 25]. Field tests look promising; Honda introduced the FCX Clarity in 2008, a PEMFC car fueled with compressed hydrogen (700 bar) and a range of about 500 km. General Motors reports having reached 100 000 miles with a vehicle in their 119-vehicle fleet and Honda has demonstrated operation of fuel cells down to -20°C [42, 43].

Chapter 3

PEMFC Degradation Mechanisms

In order to increase the life time of fuel cells it is important to understand what degrades performance and life time. The degradation mechanisms, a part of the general concept of aging, are closely linked to the operating conditions in the fuel cell, some can be controlled, others not [25]. Figure 2.8 shows the typical voltage losses in a PEMFC. However, this schematic is only valid for a fuel cell with pristine fuel cell components. As the fuel cell ages, the losses increase and the polarization curve will change, many factors are involved in this process. In this chapter we again address each component in the fuel cell and degradation mechanisms affecting those components, secondly we look at how external factors influence these mechanisms, and finally focus on the operating conditions.

3.1 PEM Degradation Mechanisms

The PEM is one of the main factors limiting the lifetime of a fuel cell stack. The origins of the degradation mechanisms are of both physical and chemical nature and both are equally important to understand. This brief survey presents the different mechanisms for degradation found in the literature and mitigation strategies to improve the lifetime of the PEM.

3.1.1 Physical Degradation

Physical degradation or degradation of the structure of the PEM is caused by for example heat, pressure, and drying. As an example, pinholes, small holes formed in the membrane cause gas flow between anode and cathode. This not only decreases the efficiency of the fuel cell, but might also cause short circuit, and the mixing of hydrogen and oxygen can be a dangerous combination. Pinholes can arise from dry spots, which cause shrinkage and expansion of the PEM, or from freezing the fuel cell. A PEM is more prone to develop pinholes after long use; stiffness and loss of backbone material are underlying causes [44, 45]. To avoid pinholes, a thicker membrane can be used, but the trade-off is a lower proton conductivity [46].

"Hot-spots" is the term for a mechanism when uneven distribution of heat speeds up the chemical degradation. Physical degradation and chemical degradation are linked; chemical

degradation can lead to mechanical failure. The situation is complex; if one spot is hotter than another the dissociation at the anode and the recombination at the cathode are faster, producing even more heat. Hot-spots can cause either drying, by increased evaporation, or flooding of the PEM. In the long term, these processes may create pinholes, see above [47].

Apart from the secondary effects as described above, subfreezing temperatures do not affect the PEM degradation, but do have an effect on the proton conductivity [48]. Degradation mechanisms during freeze/thaw cycles are related to the catalyst layer and delamination of the interface between the GDL and the PEM [49]. For an extensive report on mitigation strategies on fuel cell freezing see Pesaran *et al.* [50].

3.1.2 Chemical Degradation

The harsh chemical environment and the potential at the anode and cathode can drive unwanted chemical reactions. Radicals such as hydroxyl and peroxyl (·OH and ·OOH), formed on the cathode side, can attack both the carbon support and the PEM [51]. If these radicals attack the fluorinated backbone they form HF (hydrogen fluoride), which in turn breaks down the PEM even further. There are two suggested pathways to the hydroxyl and peroxyl radicals, outlined below [40].

Peroxide

On the cathode side, where water is formed, there will also be hydrogen peroxide as a result from the stoichiometry of the ORR on the cathode electrode (see equation 3.1) [52].

$$2H^+ + O_2 + 2e^- \rightarrow H_2O_2 \tag{3.1}$$

This product is dependent on the number of available catalyst sites. The peroxide concentration is drastically increased if the number of available sites is low [53, 54]. This can be a secondary process after the catalyst layer has lost performance due to degradation.

Metal ions

Formation of radicals through the peroxide pathway can be chemically induced by exposing the PEM to metal ions and hydrogen peroxide. This is referred to as Fenton's test and is an accelerated aging test. For fuel cells with stainless steel BPP these are the primary source for metal ions. The environment at the BPP is as discussed earlier very acidic (due to the H_3O^+ ions formed at the anode side), and easily corrode the plates. The second pathway is called the direct pathway, where protons and oxygen are directly converted into radicals with the help of the Pt catalyst.

Metal ions also hinder the proton conductivity; all metal ions have lower conductivity than protons in the PEM [55]. Furthermore, Pozio *et al.* suggests that iron from the BPP, by binding to the PEM, form radicals that attack the backbone [56]. The result is a high concentration of fluoride ions in the cathode outlet water; one mitigation strategy is to use more stable BPP.

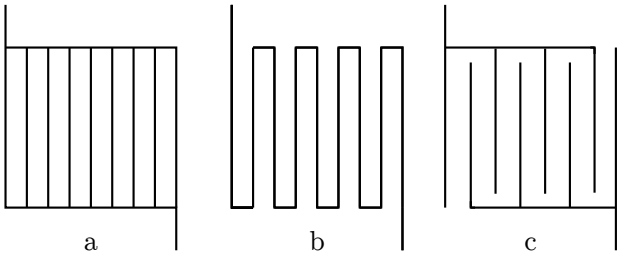

Figure 3.1: Basic flow geometries: a) parallel, b) serpentine, and c) interdigitated flow patterns.

Reformate and hydrocarbons

There is no evidence that the PEM is affected by the reformation products. De Bruijn *et al.* report that the parameters most important for PEM degradation are cycling of voltage, humidity and operating temperature [40]. The reformation products CO, CO_2 and hydrocarbon residues are more prone to affect the catalyst and carbon support. The carbon support is the chemically weak point at the three phase boundary (reactant gas, catalyst and electrolyte) and thus the material easiest corroded.

3.1.3 Water Management

The PEM needs to be hydrated to yield a good proton transport. However, too much water can flood the electrodes limiting the transport of reactant gas to the catalyst. In a PEMFC water is produced on the cathode side and may back-diffuse to the anode side. For an *in situ* study of water management, Ludlow *et al.* used neutron imaging to give insight into the dynamics of water in a working fuel cell [57]. Changing the hydration level induces volume changes in the PEM and this affects both the PEM and the electrodes mechanically.

For water management some engineering parameters are important. One is to control the humidity of the incoming gas; often by recovering the waste water from the cathode side and recirculating. Another way to improve water management is by the flow channel geometries in the BPP. For example, for the interdigitated channel flow pattern (figure 3.1c) the water is both supplied and removed by both convection and diffusion as opposed to the parallel (3.1a) and serpentine (3.1b) patterns where diffusive transport is governing [58].

3.1.4 Fuel Starvation

Fuel starvation occurs mainly when not enough fuel is supplied to complete the reaction at the anode. While the gas supply to individual cells in a stack can vary, all cells must produce the same current when coupled in series. The result is a rise in anode potential and in some severe cases the carbon support can be consumed as fuel [59]. Fuel starvation also arises from trying to minimize the waste of fuel by not supplying a surplus. Fuel starvation mainly changes the potential of the anode and thereby promotes side-reactions [25].

Some different mechanisms arise when starving the cathode gas stream. At non steady-state flow conditions the oxygen flow reacts slower to changes due to the lower diffusivity in the electrode. Also, at high current densities the reaction kinetics is mass transport limited. Because of the limited diffusivity of oxygen a high stoichiometry on the cathode side increases the current density considerably [60]. Using pure oxygen on the cathode side

provides a higher performance compared to using air. This is due to a choking effect of nitrogen, even though air contains more than enough oxygen to carry out the reaction [58].

3.1.5 Load Cycles

Varying the load changes not only affects the reaction rates at the anode and cathode, but also the potential and the water production. Fast variations are most stressful for the fuel cell and steady-state conditions are always preferred. Generally, open circuit potential (OCP), where fuel is supplied but no load is applied, should be avoided. OCP creates a high potential between the anode and cathode that accelerate all types of chemical degradation. In practical applications with a large variation of load, the fuel cell would benefit from being hybridized with a battery to buffer these large load variations. Also, fast load change can lead to fuel starvation and a reverse current causing carbon corrosion [61]. Other conditions affecting the lifetime of the PEM are temperature and relative humidity, which can induce mechanical stress causing pinholes and micro cracks, see 3.1.1 [47].

3.2 Electrode Degradation Mechanisms

Increasing the durability of the electrodes is a key factor to make PEMFC a competitive power source. The electrodes have several important tasks in the fuel cell and different types of degradation will affect these tasks differently. The performance of the MEA is dependent on the kinetics of the electrode reaction, the number of active sites, the current distribution, and mass-transport. Today, a *state-of-the-art* MEA has high power density even with a low catalyst loading, but is hampered by aging and the accompanying degradation of performance.

The primary degradation mechanisms of the electrocatalysts/electrodes are dissolution and sintering of the catalyst particles, corrosion of the carbon support material and the proton conducting matrix within the electrode layer, and induced chemical or morphological changes from poisoning. Some of the observed structural changes to the electrocatalyst are sintering which reduce the available catalytically active surface area, compositional alteration of the alloy catalysts altering the reaction mechanism, and movement of the catalyst material in the electric field potential. Poisoning can occur from dissolved species from other components within the fuel cell, such as the BPP or the gaskets or from fuel or air pollution, such as CO poisoning from reformate or salt from a marine environment [25, 62].

3.2.1 Electrocatalyst Stability: Sintering and Pt Particle Dissolution and Migration

One of the major mechanisms for the loss of active area of the electrocatalysts is the Pt or Pt alloy particle sintering [25, 62]. Sintering occurs when the well-dispersed catalysts agglomerate into larger, more thermodynamically stable particles. The particle growth can be atomic where individual atoms move (Oswald ripening), which usually occurs through dissolution and re-precipitation in the fuel cell environment or an entire catalyst particle can move and merge with another particle (coalescence) [63]. When Pt particles migrate on the support either through Ostwald ripening or coalescence the average supported Pt

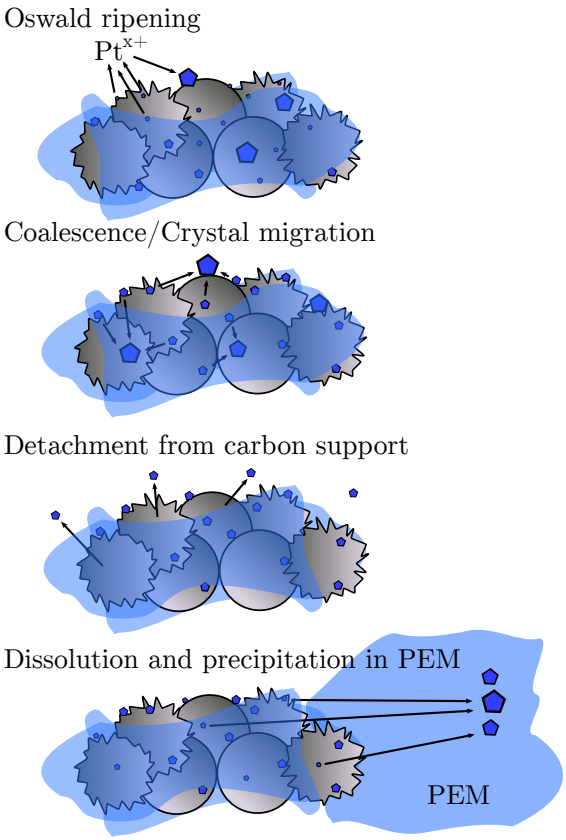

Figure 3.2: The different mechanisms of sintering and migration of catalyst material in the electrode of a PEMFC [64].

particle size increase, reducing the electrochemically active surface area, leading to a reduced performance of the cell.

Another loss of Pt can occur through oxidized Pt species dissolving in the aqueous environment, detaching from the support and re-precipitating either on defect sites on the support, within the ionomer layer or within the membrane itself. The latter leads to the development of this Pt band within the membrane [25, 64]. With high potential over the electrodes and membrane, the platinum on the cathode can form platinum ions or platinum complexes and migrate into the membrane towards the anode until it reaches a higher concentration of hydrogen where it is reduced to metal nano-particles within the membrane [63, 65, 66], precipitating as small particles within the membrane [64, 67]. This decreases the performance of the cell due to loss of active catalyst sites. The mechanisms involved with Pt particle sintering and dissolution re-precipitation are summarized in figure 3.2.

It is known that Pt can become oxidized in an aqueous environment depending on the pH and potential, as can be seen in the Pt/water Pourbaix diagram [25, 68]. Above 1.18 V, a diffuse mono-layer thin oxide layer has been seen on Pt. However, when cycling to lower potentials (<0.5 V) this oxide layer can be reduced. Pt has been found to be slightly soluble under conditions found in a PEMFC, but the soluble species has not yet been identified [25]. There are several operational modes which have been shown to exacerbate the sintering of the Pt particles including repeated start-stop cycles and extended operation at high potentials and OCP [61]. At OCP, under acidic conditions, PtO_2 is known to be stable,

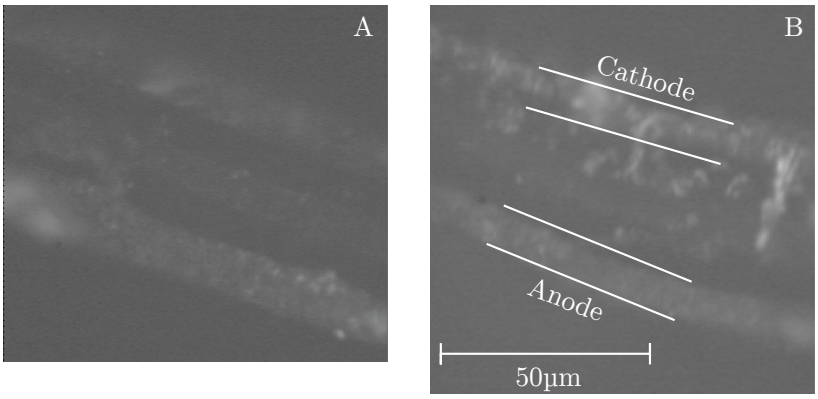

Figure 3.3: A: Unused membrane with electrodes. B: Analysis of a degraded PEM with electrodes, after PEM failure (Post-mortem). The cathode has sustained considerable carbon corrosion. The cathode components (light gray) are dispersed all the way into the PEM. The carbon migration into the PEM is confirmed using micro-Raman [37]

and this condition should therefore be avoided [25].

Approaches to minimize the loss of electrochemically active surface area have focused on changing the characteristics of the catalyst or modifying the support [69, 70]. For example, it has been shown that alloying the Pt with cobalt helps resist dissolution even though the average particle size is larger and thus the active surface area is smaller [71]. Modifying the support with a metal oxide has also been shown to reduce the sintering of the Pt particles without reducing their activity [21].

To mitigate catalyst poisoning in reformat systems, the Pt catalyst is alloyed with ruthenium (Ru) to improve the CO-oxidation properties of the catalyst. However, Ru is more readily oxidizable than Pt, and forms a soluble $Ru(OH_2)$ above 0.6 V and pH 3 [72]. A potential mechanism is preferential loss of Ru under potential cycling, leading to a diminished tolerance for CO poisoning, and thus an overall loss in performance [73]. In long term stack testing Ru particles were found on the anode/membrane interface within the membrane [74].

3.2.2 Electrode Corrosion

Carbon support corrosion or carbon oxidation is the process where the carbon support for the catalyst is oxidized and broken down during fuel cell operation [40]. Figure 3.3 is a light microscope picture of a degraded commercial MEA. A light gray band corresponds to the anode, while the cathode band is not as well defined, indicating the breakdown of the catalyst layer. This MEA had lost 42% of its initial performance during the lifetime testing [37].

Oxidation of the catalyst support can also be promoted on the anode side by high potentials and low relative humidities [21]. This can occur when the fuel is unevenly distributed and not enough hydrogen is available locally (fuel starvation). This drives the potential in negative direction until these reactions can take place, similar to a shutdown fuel cell [62]. Schultze *et al.* [75] have shown that the added Polytetrafluoroethylene (PTFE) degrades preferentially on the anode side of a working fuel cell. This can lead to a decrease in gas permeability due to liquid water trapped in the pores.

3.3 External Factors

3.3.1 Poisoning

Poisoning is when the activity of the catalyst is diminished upon exposure to the substance. For fuel cells, this is often caused by impurities in the reactant gas streams, but also from degradation products from other cell components such as gaskets and BPP [25]. The poisoning effect is temperature dependent and high temperature PEMFC (200°C) are not affected in the same way as low temperature PEMFC (80°C).

Fuel impurities

The source of hydrogen fuel impacts the impurities found in the feed stream. Both reformation of hydrocarbons and water electrolysis can produce hydrogen with high purity, but the cost is a low efficiency. Electrolysis systems that use salt water or unpurified water can contain some impurities, however, usually not enough to poison the fuel cell. For reformate system, the hydrocarbons can contain sulfur and nitrogen oxides which affect both performance and durability. The most common and well-studied impurity is CO which is most abundant in reformate systems and poison the catalyst by occupying the reaction sites. Additional impurities are ammonia, hydrogen sulfide, hydrocarbons, aldehydes, mercaptans, and cyanides. As little as 30 ppm of NH_3 can cause irreversible loss of protonic conductivity in the membrane around the anode. This loss is attributed to the formation of NH_4^+. Hydrogen sulfide absorbs on the electrocatalyst surface reversibly, if the cell is allowed to go to high potentials. If not, concentrations as low as 10 ppb can have a deterious effect on performance [25].

When steam reforming hydrocarbons, traces (25 ppm - 3%) of carbon monoxide (CO) will be present in the anode gas stream. As little as 25 ppm CO blocks enough active sites on the platinum catalyst to severely slow down the anode process at 80°C. This process is reversible and adding a small amount of oxygen to the anode stream (air bleed) reduces the poisoning effect [76]. Because reformate contains high concentrations of CO_2, the power density of the fuel cell is slightly lower due to mass transport limitations [77, 78]. Alloying with ruthenium on the anode increases the efficiency of oxidizing CO to CO_2 and is therefore the popular choice for reformat systems [49, 79, 80]. The choice of catalyst also affects the activation losses [25].

3.4 PEMFC degradation

In order for the PEMFC to be able to compete with the ICE, both cost and durability of all components needs to be improved. Studies have shown that the current technology with the correct operating conditions and manufacturing techniques can reach this goal [40, 25]. To optimize the materials it is important to know the degradation mechanisms and how they affect the performance life-time of the complete fuel cell system.

Degradation mechanisms are coupled to the operating parameters. For example cycling the load rapidly, operating at low temperatures or start/stop cycling degrade the components faster than steady-state operation at constant temperature. To accurately predict the life

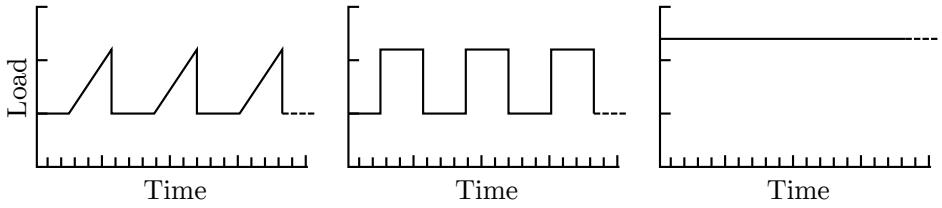

Figure 3.4: Three different operating schemes, load decides all other parameters such as reactant flow rates, cell voltage etc. These operating schemes are designed to investigate how either steady-state or dynamic load affect the life of the components and complete fuel cell system.

time or inducing stress to find weak components or design one needs to consider which operating scheme to apply.

3.5 Operating conditions

The term "automotive conditions" are often applied when a system design is intended for transport application. These include cars, trucks, construction equipment, marine applications and auxiliary power and the basic requirements involve high power density, fast change of load idle operation at OCV. For propulsion application (cars, trucks) the load cycle is often dynamic such as saw-tooth (Figure 3.4)

Accelerated testing intends to slow down development time, material screening and lowering costs. These are typically done by exaggerating a parameter. Examples of *in situ* accelerated aging schemes are open-circuit-voltage; creating radicals under the high potential and readily available fuel, fuel starvation, causing reversal of the fuel cell in areas with insufficient fuel. The most commonly used *ex situ* accelerated degradation scheme is Fenton's solution or Fenton's reagent. The material is treated with a solution of hydrogen peroxide and iron catalyst oxidizing ferrous iron(II) to ferric iron(III). The product yield two radicals; one hydroxyl radical (·OH) and one peroxide radical (·OOH). According to literature, the accepted theory is radical attack on the back-bone creating a so called unzipping effect of the polymer chain.

3.5.1 Fuel cell shutdown

When shutting down a PEMFC it is important to consider what will happen with the remaining reactants. The anode and cathode still contain fuel and water, the potential between the anode and cathode will have OCP. To stop the reactions, one option is to purge the anode with inert nitrogen. This however requires nitrogen to be stored on-board, making the system more complex. If the exhaust is closed, the hydrogen will remain on the anode and slowly diffuse through the membrane to the cathode. Tang *et al.* studied the reactions occurring when the exhaust of the fuel cell is left open after shutdown. Air will diffuse into the anode of the fuel cell creating an environment where several unwanted reactions will take place [81].

Chapter 4

Analysis Methods

Analysis of the degradation of the PEMFC can be done in several ways and with several techniques. Some techniques give confirmation, while others give complementary information. It is useful to divide the experiments into two categories, *in situ* and *ex situ*. *In situ* experiments are performed under operation of the fuel cell, as the degradation is taking place, while *ex situ* experiments, are performed after the aging experiment has been performed. Some methods can be used both *in situ* and *ex situ*, others only in the latter mode, those requiring special conditions such as ultra-high vacuum.

This work focuses on vibrational spectroscopy, more exactly Raman spectroscopy. In addition, electrochemical impedance spectroscopy (EIS) was used to monitor the health of the fuel cell during the aging experiments. X-ray photo-electron spectroscopy (XPS) and transmission electron spectroscopy (TEM) were used to confirm and complement the results from the Raman spectroscopy experiments.

4.1 Vibrational Spectroscopy

Vibrational spectroscopy is a family of spectroscopy methods studying the molecular vibrations, rotations and other low-frequency modes in the material. The molecular vibrations are excited by broad or narrow band photon energy sources (often a laser) from the infra-red spectrum up to ultra-violet. When a photon hits an electron in the material, different scenarios can occur; the material can absorb the energy robbing the broad energy spectrum of some frequencies (e.g. IR spectroscopy), the photon can scatter against the material elastically without energy loss (Rayleigh scattering), or scatter in-elastically with energy loss (e.g. Raman spectroscopy), see figure 4.1 [82].

4.1.1 Raman Spectroscopy

In-elastically scattered light in the visible (vis) and ultra-violet (UV) range is referred to as Raman scattered light. This vibrational scattering was first observed by Sir Chandrasekhara Venkata Raman in 1928 and gave rise to a new tool of non-destructive material analysis. Energy from incoming photons is absorbed by the electrons in the material and the electrons are transferred to a higher energy state. When the electrons return to the

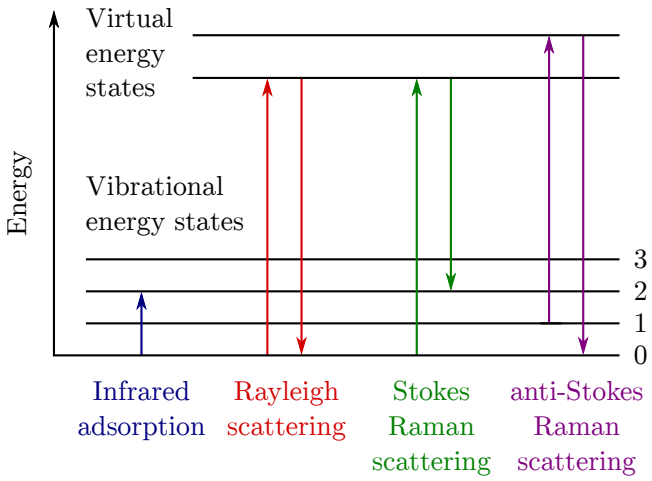

Figure 4.1: Raman scattering, as opposed to Rayleigh scattering, is inelastic which means that the energy of the incoming light and the emitted light are of different wave lengths.

original state or an intermediate state the excess energy is emitted as a secondary photon. This is as opposed to Rayleigh scattering where the energy of the secondary photons have the same energy as the excitation source, but with changed intensity [82].

Both Stokes Raman scattering and anti-Stokes Raman scattering occur in a material exposed to light, however, Stokes Raman scattering have a higher probability than anti-Stokes as the number of molecules in the ground-state is larger than the number in excited state. The Stokes and anti-Stokes scattering spectra contain the same information and both are equally useful (figure 4.1).

The scattering process occurs for all ranges of electro-magnetic energies and materials, for a more controlled Raman process the use of a narrow energy laser is preferred. Any laser source from vis to UV is suitable; in literature the most commonly used ones are Ar-ion (green, 514.5 nm) He-Ne (red, 632.8 nm) and Nd-YAG (infra-red, 1064 nm). The intensity needs to be controlled in order to preserve the material and laser intensities in the milliwatt range are common [83].

With the short wave-length, Raman has the benefit that it can be combined with a microscope to measure local properties of the material. This setup is often referred to as micro-Raman and the sample volume of one of these setups are in the order of a few cubic micro meters. Using a micro-Raman setup it is also possible to yield small volume sampling in the fuel cell in the order of 5 μm [84]. The confocal Raman spectroscopy adopts the benefits of confocal microscopy where only a small volume or surface of the sample is illuminated and sampled. This gives a very small and controlled sample volume compared to wide-field microscopy where a large area or the whole sample is illuminated, and a small volume sampled. A pinhole is placed in the focal path of the laser beam, rejecting out of focus light, see figure 4.2. The signal-to-noise ratio is also improved using confocal technique [85].

For fuel cell analysis, Raman spectroscopy is in particularly suitable for observing carbon (GDL, MPL), the PFSA-membrane and water in a fuel cell (figure 4.3). As Raman spectroscopy is a non-destructive analysis method, it is possible to perform *in situ* experiments

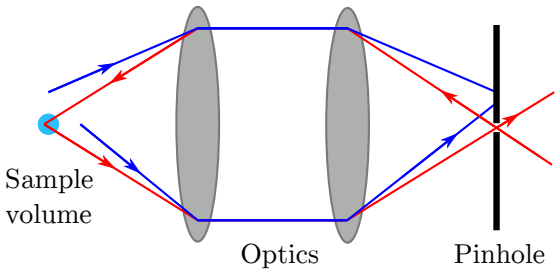

Figure 4.2: The principal of confocal microscopy, the illumination of the sample is focused into a small spot using optics and pinholes (red lines). All scattered light originating from any other parts of the sample are blocked by the same pinholes (blue lines).

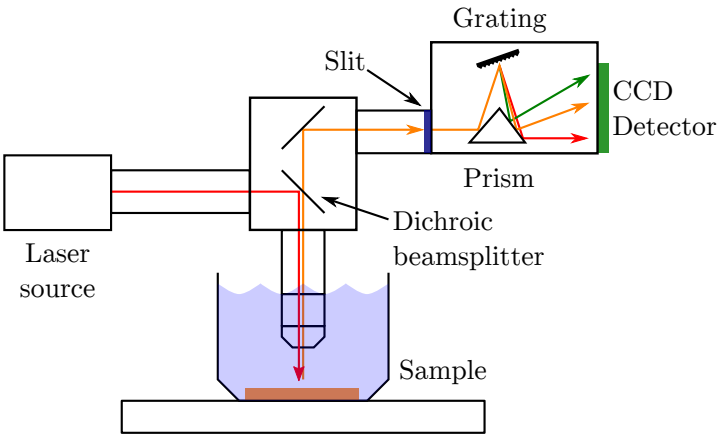

Figure 4.3: Schematics of a simple micro-Raman setup. A Raman spectroscope setup combined with an immersion microscope makes a powerful combination for both *in situ* and *ex situ* analysis. Micro-Raman setups are often coupled with an imaging part using the microscope optics for focusing and imaging (not in schematics).

on operating fuel cells and post-mortem analysis to determine the changes in structure and composition before and after aging experiment [35].

4.2 Electrochemical Impedance Spectroscopy (EIS)

Electrochemical impedance spectroscopy (EIS) is a real time measurement possible to perform *in situ* during operational mode. The aim of an EIS measurement is to determine the type and magnitude of the resistances in the fuel cell. The most common analysis span an entire fuel cell from one current collector (BPP) to the other, it is also possible with special techniques to measure only on certain components or over multiple cells, but with reduced traceability of the location of the resistances. The basic principle of EIS and components required are described in figure 4.4.

4.2.1 Electrical Component Modeling of EIS

To extract the specific resistance or capacitance of one specific component, for example the membrane, an equivalent circuit model must be applied. The model use common electrical components such as resistors (R), capacitors (C), and inductors (L). To model diffusion and mass transport it is necessary to introduce more advanced elements such as phase dependent resistors, Warburg impedance (Z_W), in the circuit model [86]. Figure 4.5 show a

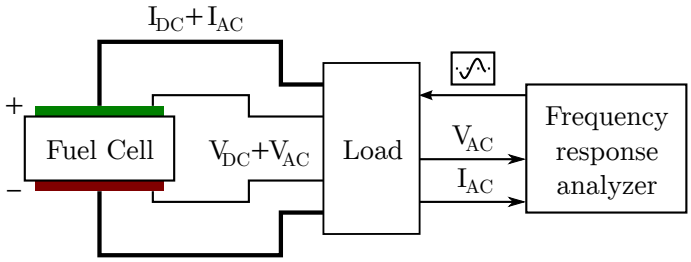

Figure 4.4: The principle of EIS. The frequency response analyzer generates an AC-perturbation on top of the DC load of the fuel cell. The voltage sense leads measure voltage over one or more cells in a stack ($V_{cell} = V_{DC} + V_{AC}$). The main cell leads measure the current over the whole fuel cell stack ($I_{cell} = I_{DC} + I_{AC}$). Finally, the small AC voltage (V_{AC}) and current (I_{AC}) is measured by the frequency response analyzer.

		Definition	Impedance
Resistor		$V = I \cdot R$	$Z_R = R$
Capacitor		$I = C\frac{dV}{dt}$	$Z_C = \frac{1}{j\omega C} = -\frac{j}{\omega C}$
Inductor		$V = L\frac{dI}{dt}$	$Z_L = j\omega L$

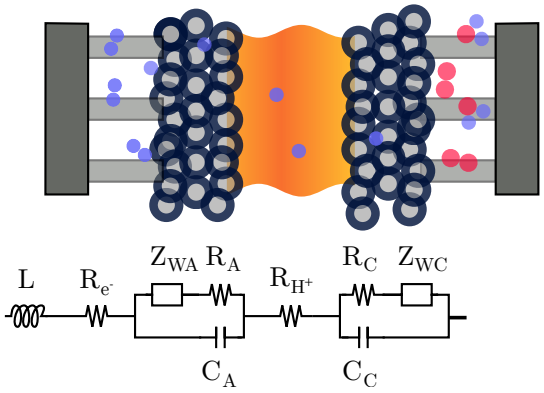

Figure 4.5: An example of an equivalent circuit model for a PEMFC cell. L is the induction in the wiring for the instruments, to and from the fuel cell. R_{e^-} is the bulk contact, the resistance for electron to and from the active layer. Z_{WA},R_A, and C_A together represent the mass transport, resistance and capacitance in the anode electrode, a similar circuit is also represent the cathode. Finally, the resistance R_{H^+} is the proton transport resistance, typically the largest resistance in the PEMFC.

typical model of a single cell, this model requires several measurements with high precision, preferably without load to minimize the measurement errors.

4.2.2 EIS applied to PEMFC

EIS can reveal several PEMFC problems; flooding of the electrodes as increased mass transport resistance in the high frequency zone (Warburg impedance), loss of catalyst activity as lowered capacitance, or complete failure of the cell. During fuel cell testing, EIS is performed on a regular basis. EIS measurements can be performed either during steady-state load or at OCP, an external AC-voltage is applied over the fuel cell and the response is measured. To complete the measurement, a sweep of frequencies is recorded, typically by a 10 mV perturbation from 10 mHz to 10 kHz [33].

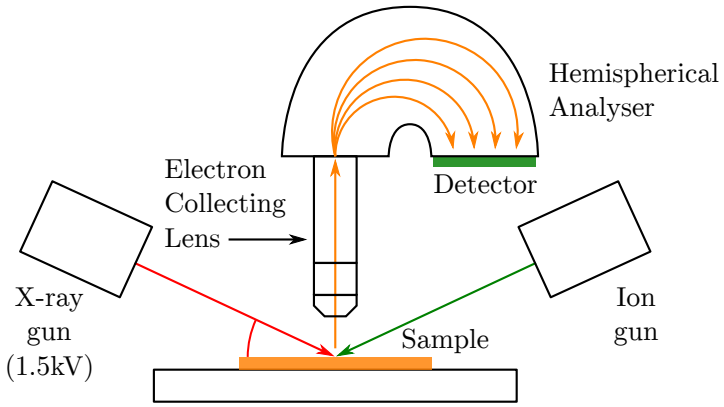

Figure 4.6: Traditional XPS Setup, the sample is excited by high energy electrons (1.5 kV), non-elastically scattered electrons (photo-emitted electrons) from the surface region of the sample (70-110 Å) will travel through an Electron Collection Lens into the Hemispherical Analyzer or Electron Energy Analyzer. The electrons are separated by an electric field to determine the energy of the photo-emitted electrons. An ion gun (Argon) can be used to clean the sample surface prior or during measurement. The ion gun can also be used for depth profiling.

4.3 X-ray Photo-electron Spectroscopy (XPS)

Similar to vibrational spectroscopy the molecules are in X-ray photo-electron spectroscopy (XPS) excited, but here by high energy electrons in the X-ray region (around 1.5 kV energy). The focused beam of electrons referred to as primary electrons is directed towards the sample with an inclination angle towards the sample, the detector is placed at the same angle opposite the excitation source (Figure 4.6). The detector is selective and discards the elastically scattered electrons from the electron source; only photo-emitted electrons (less energy than the excitation source) from the sample are counted. The indecent beam of electrons scatters with the electrons in the inner orbitals of the atoms of the material creating secondary electrons.

The probing depth of XPS is around 70-110 Å, due to the short reach of the secondary electrons. The detected secondary electrons detected originates from the 1s, 2s, 2p 3s etc. XPS is useful for detecting light elements as these inner orbitals are exposed and require less excitation energy to leave the orbitals.

XPS require low pressure to yield a good signal-to-noise ratio, a pressure of 10^{-6} Pa is considered standard. Recent techniques of environment XPS with various stages of vacuum allows experiments to be carried out at as high as 1 Pa at room temperature, however, the PEM-fuel cell require 40-100% humidity at 60-120°C and 10^5 Pa (1 atm), which makes this technique unsuitable for *in situ* fuel cell experiments, but suitable for more specific experiments such as observing CO oxidation on ruthenium [87].

4.4 Electron Microscopy

Scanning electron microscopy (SEM), transmission electron microscopy (TEM) and scanning transmission electron microscopy (STEM) are imaging techniques using high energy electrons to image small samples on a micrometer to sub-nano-meter level. All three techniques use focused electron beams to image the sample, some basic technical differences

gives the techniques different advantages.

SEM is used to image large areas from centimeter range down to nano-meter range. The surface is scanned with an electron beam in the energy range of 0.2-30 kV and the elastically scattered electrons, in-elastically scatted electrons, or electromagnetic radiation from the scattering is collected at angle from the indecent beam. SEM imaging require the sample to be electrically conducting to avoid electrostatic charging of the surface with adsorbed electrons, for GDL, electrode and catalyst this is not a problem, while for the PEM this becomes more difficult, but selecting a lower acceleration voltage for the electrons reduces the charging effect.

TEM is a high resolution microscopy method used to image down to sub-nano-meter level. Electrons in the energy range of 100-300 kV are directed with high precision magnetic lenses and apertures to focus the electron beam onto the whole sample. It is also possible to scan the sample using electromagnets to focus the beam on a small spot on the sample and scan over the surface (STEM).

For PEMFC, SEM and STEM are interesting as they can be combined with energy dispersive X-ray spectroscopy (EDX) or electron energy loss spectroscopy (EELS) to not only image the surface, but also collect elemental information about the surface. All electron microscopy techniques require vacuum (10^{-4} Pa or lower) in the sample chamber to maintain the mean free path for the electrons, which makes these techniques suitable for *ex situ* analysis. SEM and (S)TEM are excellent tools to characterize the active layer, degradation of electro catalyst, carbon support, and catalyst migration into the PEM [37, 84, 88].

Chapter 5

Summary of Papers and Related Work

5.1 Paper I

In this study we compared material aged in a real fuel cell for 1500 h with material aged under controlled artificial conditions for 24 h. The purpose was to compare the degradation mechanisms of the artificial scheme with the material aged in a real fuel cell to determine if it is possible to simplify aging studies. The artificial degradation method chosen was Fenton's solution deposited by vapor. Both material aged under real and artificial conditions showed visible signs of degradation. Confocal Raman spectroscopy was the tool used to determine the chemical degradation. The PFSA-membrane consist of two units, one backbone and numerous side chain groups. The backbone is built by CF_2 units in a long chain. The side chain have a chemical structure consisting of CF_2, C-O-C and C-S-O units. The main conclusion of the paper was that the degradation of the PEM is due to two mechanisms; the first breaking down the back-bone, thus compromising the stability of the PEM, the second removing the proton conducting end-groups, resulting in an increased resistance and thereby lower efficiency. Raman spectroscopy can indeed detect both these degradation mechanisms, however, while the PEM degraded in a real fuel cell show signs of both these mechanisms, the material degraded under artificial conditions show only signs of back-bone degradation. The results are summarized in two graphs. The lower Raman intensity of C-S, C-O-C and S-O indicate that the side chain groups of the PEM are cut of from the backbone during the degradation. The artificially degraded material does not show any Raman spectral features due to this type of degradation.

5.2 Paper II

Here the analysis goes deeper into the membrane. The focus was on the structural changes even leading to visible degradation of the PEM. The degradation is greater on the cathode side, as expected from the literature. The physical degradation is also detected by Raman spectroscopy in the lower energy region (1100-1800 cm^{-1}). The Raman active bonds for the carbon-based components have two peaks at approximately 1330 cm^{-1}(D-mode) and 1600 cm^{-1}(G-mode) [37, 83]. The ratio of intensity of these peaks indicate which carbon

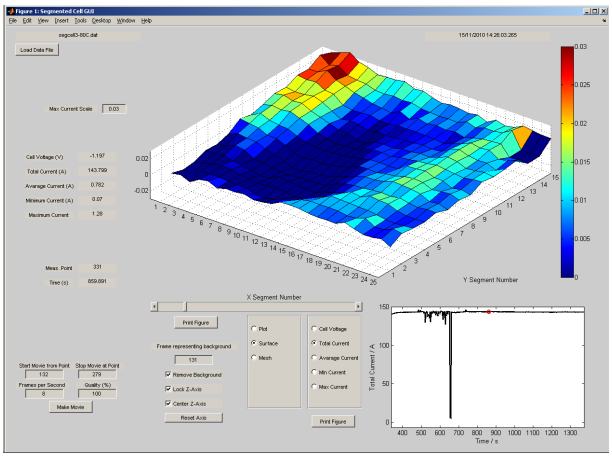

Figure 5.1: Custom made software to analyze data from segmented cell.

structure is more favored in the material. Certain types of degradation may be prone to degrading one type more than another which results in change in the intensity ratio. An increased carbon signal from the cathode side of the PEM is indicative of carbon support corrosion. This is in agreement with the microscope images.

5.3 Paper III

This paper gives insight on how the carbon support (GDL and MPL) move inside the MEA during aging. Based on the results of articles 1 and 2, and with the aid of XPS, we investigated the changes in the carbon in the interface between the PEM and the active layer. After separating the PEM from the carbon support, we measured the XPS spectra on both sides of this interface. This yields 4 measurements on each MEA, two on the anode and two on the cathode. Comparing the C-C content and the C-F content we can determine if the measurement is in the GDL (0 mass-% C-F) or in the MEA (0.033 mass-% C-F). In the same XPS measurement we can also see the Pt content and distribution. The conclusion made is that while the total Pt content remains the same throughout the aging, the distribution becomes broader, stretching further into the MEA and further out into the carbon support.

5.4 The Segmented Cell

PEMFCs can exhibit an uneven current distribution within a single cell under operation. The current is, however, measured as the average current distribution over the entire active surface and gives no information about heterogeneities. Factors for heterogeneities can be concentration gradients or stagnant zones, pressure drop, temperature gradients or "hot-spots", local flooding or drying etc. and can severely lower the life-time and performance. Here we utilized a custom made current distribution card with 375 measurement segments over the 200 cm^2 cell area. By changing parameters such as stoichiometry (fuel starvation, stagnation), humidity (drying/flooding), CO-content (poisoning) and different flow patterns we revealed important design parameters and poisoning mechanisms. The study was focused in particularly on the CO-poisoning effect for auxiliary power unit reformate PEMFC.

Chapter 6

Future Outlook

A licentiate thesis is commonly considered to be written when one has reached about half way down the road to a PhD, for me this is the end of that chapter as I have decided to pursue another career. Nevertheless, the time I have spent on this work has been very rewarding giving me skills for life. Working in the automotive sector I see a bright future for fuel cell technology; Improving the life time of the components, reducing component cost, and last but not least, legislation to promote environmental friendly technologies all play key roles for a successful market introduction.

Raman spectroscopy is an excellent technique to measure the chemical composition of PEMFC material. With the addition of a confocal microscope set up it enables tracking local degradation inside the membrane. Furthermore, using *in situ* confocal Raman spectroscopy to study hydration and degradation mechanisms of the PEM has great potential to further reveal the degradation mechanisms under operation. This method is one of the few *in situ* techniques able to be used on a real fuel cell under normal operating conditions, and the ability to study the chemical degradation with a large spatial resolution (on the order of micro meters) makes it one of a kind.

In summary, the low temperature PEMFC has great potential in the transportation sector. Light weight, compactness, and high efficiency, gives the PEMFC a clear place in situations when batteries are not enough. Another great feature of PEMFC is the ability to use hydrocarbon based fuel sources with a reformer. This makes the technology potentially successful with both direct hydrogen, renewable, and non-renewable fuel sources.

Acknowledgments

I want to thank my supervisor Patrik Johansson for supporting and encouraging me to keep going with this thesis. The road to finalizing this work has not been completely linear, but with Patrik's motivating words and sound advice we managed to get all three articles finished and submitted, and this licentiate thesis finished.

I will remember Per Jacobsson with nothing but love and respect in my heart. Despite all his positive spirit and life energy, he is not with us anymore. He was the most inspiring person I have ever met, always encouraging to go further and to pursue your heart's desires. A big part of me wanted to finish this thesis for him.

I would like to thank my colleagues at Volvo Technology for the support and creating a great everyday workplace. During the later writing part of this thesis I have been working for Sigma Technology, my managers at Sigma have been very supportive and made it possible for me to take time to finalize this work.

This work was funded by the European FP7 program DECODE (213295). Some of the materials used was provided by PowerCell AB, a special thank you to Andreas Bodén, whom helped providing the materials. A warm thank you goes out to the partners in the DECODE-project that helped, inspired, and ran the project, now resulting in this thesis.

Finally, I'm sending my warmest gratitude to my friends and especially my girlfriend whom have always encouraged me to develop and take new steps into the unknown. There are many valuable life lessons to be learned, and we have our whole lives to learn them.

Bibliography

[1] S. L. Postel, "Water for Food Production: Will There Be Enough in 2025?," *BioScience*, vol. 48, pp. 629–637, 1998.

[2] M. Kummu, D. Gerten, J. Heinke, M. Konzmann, and O. Varis, "Climate-driven interannual variability of water scarcity in food production potential: a global analysis," *Hydrology and Earth System Science*, vol. 18, pp. 447–461, 2014.

[3] "BP Statistical Review of World Energy." `http://www.bp.com/content/dam/bp/pdf/statistical-review/statistical_review_of_world_energy_2013.pdf`, 2013. Last accessed 2014-02-23.

[4] E. Cartlidge, "Saving For a Rainy Day," *Science*, vol. 334, pp. 922–924, 2011.

[5] A. Demirbas, "Combustion characteristics of different biomass fuels," *Progress in Energy and Combustion Science*, vol. 30, pp. 219–230, 2004.

[6] D. Tilman, R. Socolow, J. A. Foley, J. Hill, E. Larson, L. Lynd, S. Pacala, J. Reilly, T. Searchinger, C. Somerville, and R. Williams, "Beneficial Biofuels - The Food, Energy, and Environment Trilemma," *Science*, vol. 325, pp. 270–271, 2009.

[7] M. Hubbert, "Nuclear Energy and the Fossil Fuels." Presented before the Spring Meeting of the Southern District Division of Production, American Petroleum Institute, 1956.

[8] L. Fulton and G. Eads, "IEA/SMP Model Documentation and Reference Case Projection." `http://www.wbcsd.org/web/publications/mobility/smp-model-document.pdf`, 2004. Last accessed 2014-02-27.

[9] K. Aleklett, M. Höök, K. Jakobsson, M. Lardelli, S. Snowden, and B. Söderbergh, "The Peak of the Oil Age - Analyzing the world oil production Reference Scenario in World Energy Outlook 2008," *Energy Policy*, vol. 38, pp. 1398–1414, 2010.

[10] C. Lutz, U. Lehr, and K. S. Wiebe, "Economic effects of peak oil," *Energy Policy*, vol. 48, pp. 829–834, 2012.

[11] G. Bettini and L. Karaliotas, "Exploring the limits of peak oil: naturalising the political, de-politicising energy," *The Geographical Journal*, vol. 179, pp. 331–341, 2013.

[12] C. Kerschner, C. Prell, K. Feng, and K. Hubacek, "Economic vulnerability to Peak Oil," *Global Environmental Change*, vol. 23, pp. 1424–1433, 2013.

[13] IEA, "Key World Energy Statistics." `http://www.iea.org/publications/freepublications/publication/KeyWorld2013.pdf`, 2013. Last accessed 2014-02-25.

[14] H. Idriss, "Ethanol Reactions over the Surfaces of Nobel Metal/Cerium Oxide Catalysts," *Platinum Metals Rev.*, vol. 48, pp. 105–115, 2004.

[15] R. B. Gupta, *Hydrogen Fuel: Production, Transport, and Storage*. Taylor & Francis Group, 2009.

[16] V. S. Bagotsky, *Fuel Cells: Problems and Solutions*. John Wiley & Sons Inc., 2009.

[17] Hydrogen Association, "Hydrogen Safety." `http://www1.eere.energy.gov/hydrogenandfuelcells/pdfs/h2_safety_fsheet.pdf`, 2010. Last accessed 2014-05-25.

[18] "PowerCell - PowerPac." `http://www.powercell.se/wp-content/uploads/2013/11/PowerPac.pdf`, 2013. Last accessed 2014-04-27.

[19] M. Henell, "PowerPac: Swedish fuel cell developer PowerCell unveils cleanest and most energy efficient fuel cell system yet to convert road diesel to electricity." `http://www.powercell.se/2013/05/`, 2013. Last accessed 2014-04-27.

[20] D. Hülsebusch, J. Ungethüm, T. Braig, and H. Dittus, "Multidisciplinary simulation of vehicles," *ATZ worldwide*, vol. 111, pp. 50–55, 2009.

[21] R. Borup, J. Davey, F. Garzon, D. Wood, and M. Inbody, "PEM fuel cell electrocatalyst durability measurements," *Journal of Power Sources*, vol. 163, pp. 76–81, 2006.

[22] S. G. Kandlikar and Z. Lu, "Thermal management issues in a PEMFC stack - A brief review of current status," *Applied Thermal Engineering*, vol. 29, pp. 1276–1280, 2009.

[23] S. Zhang, X.-Z. Y, J. N. C. Hin, H. Wang, K. A. Friedrich, and M. Schulze, "A review of platinum-based catalyst layer degradation in proton exchange membrane fuel cells," *Journal of Power Sources*, vol. 194, pp. 588–600, 2009.

[24] D. Wu, S. Paddison, J. Elliott, and S. Hamrock, "Mesoscale Modeling of Hydrated Morphologies of 3M Perfluorosulfonic Acid-Based Fuel Cell Electrolytes," *Langmuir*, vol. 26, pp. 14308–14315, 2010.

[25] R. Borup, J. Meyers, B. P. Y. Kim, R. Mukundan, N. Garland, D. Myers, M. Wilson, F. Garzon, D. Wood, P. Zelenay, K. More, K. Stroh, T. Zawodzinski, J. Boncella, J. McGrath, M. Inaba, K. Miyatake, M. Hori, K. Ota, Z. Ogumi, S. Miyata, A. Nishikata, Z. Siroma, Y. Uchimoto, K. Yasuda, K. Kimijima, and N. Iwashita, "Scientific Aspects of Polymer Electrolyte Fuel Cell Durability and Degradation," *Chemical Reviews*, vol. 107, pp. 3904–3951, 2007.

[26] V. Arcella, A. Ghielmi, L. Merlo, and M. Gebert, "Membrane electrode assemblies based on perfluorosulfonic ionomers for an evolving fuel cell technology," *Desalination*, vol. 199, pp. 6–8, 2006.

[27] J. Larminie and A. Dicks, *Fuel Cell Systems Explained*. John Wiley & Sons Ltd., 2003.

[28] E. Aleksandrova, R. Hiesgen, D. Eberhard, K. Friedrich, T. Kaz, and E. Roduner, "Proton conductivity study of a Fuel Cell Membrane with Nanoscale Resolution," *ChemPhysChem*, vol. 8, pp. 519–522, 2007.

[29] N. Economou, J. O'Dea, T. McConnaughy, and S. Buratto, "Morphological differences in short side chain and long side chain perfluorosulfonic acid proton exchange membranes at low and high water contents," *RSC Advances*, vol. 3, pp. 19525–19532, 2013.

[30] K. Schmidt-Rohr and Q. Chen, "Parallel cylindrical water nanochannels in Nafion fuel-cell membranes," *Nature Materials*, vol. 7, pp. 75–83, 2008.

[31] K.-D. Kreuer and G. Portale, "A Critical Revision of the Nano-Morphology of Proton Conducting Ionomers and Polyelectrolytes for Fuel Cell Applications," *Advanced Functional Materials*, vol. 23, pp. 5390–5397, 2013.

[32] X. Cheng, Z. Shi, N. Zhang, L. Glass, J. Zhang, D. Song, Z. Liu, H. Wang, and J. Shen, "A review of PEM hydrogen fuel cell contamination Impacts, mechanisms, and mitigation," *Journal of Power Sources*, vol. 165, pp. 739–759, 2007.

[33] X.-Z. Yuan, C. Song, H. Wang, and J. Zhang, *Electrochemical Impedance Spectroscopy in PEM Fuel Cells: Fundamentals and Applications*. Springer, 2009.

[34] W. Dai, H. Wanga, X. Yuan, J. J. Martin, D. Yang, J. Qiao, and J. Mab, "A review on water balance in the membrane electrode assembly of proton exchange membrane fuel cells," *International journal of Hydrogen Energy*, vol. 34, pp. 9461–9478, 2009.

[35] H. Matic, A. Lundblad, G. Lindbergh, and P. Jacobsson, "In Situ Micro-Raman on the Membrane in a Working PEM Cell," *Electrochemical and Solid-State Letters*, vol. 8, pp. A5–A7, 2005.

[36] N. Yousfi-Steiner, P. Mocoteguy, D. Candusso, D. Hissel, A. Hernandez, and A. Aslanides, "A review on PEM voltage degradation associated with water management: Impacts, influent factors and characterization," *Journal of Power Sources*, vol. 183, pp. 260–274, 2008.

[37] M. Holber, P. Johansson, and P. Jacobsson, "Raman Spectroscopy of an Aged Low Temperature Polymer Electrolyte Fuel Cell Membrane," *Fuel Cells*, vol. 3, pp. 459–464, 2011.

[38] P. Trogadas, J. Parrondo, and V. Ramani, "Degradation Migigation in Polymer Electrolyte Membranes Using Cerium Oxide as a Regenerative Free Radical Scavenger," *Electrochemical and Solid-State Letters*, vol. 11, pp. B113–B116, 2008.

[39] J. Sinha, "V.A.3 Cost Analyses of Fuel Cell Stacks/Systems." `http://hydrogendoedev.nrel.gov/pdfs/progress10/v_a_3_sinha.pdf`, 2010. Last accessed 2014-01-10.

[40] F. Bruijn, V. Dam, and G. Janssen, "Review: Durability and Degradation Issues of PEM Fuel Cell Components," *Fuel Cells*, vol. 8, pp. 3–22, 2008.

[41] M. Holber, A. Carlsson, P. Jacobsson, L. Jörissen, and P. Johansson, "Raman Investigation of Degradation and Ageing Effects in Fuel Cell Membranes," *ECS Transactions*, vol. 25 (1), pp. 807–811, 2009.

[42] General Motors, "Fuel Cell Equinox Tops 100,000 Miles in Real-World Driving." `http://media.gm.com/media/us/en/gm/news.detail.html/content/Pages/news/us/en/2013/Oct/1022-fc-equinox.html`, 2013. Last accessed 2014-01-14.

[43] K. Goto, I. Rozhanskii, and Y. Yamakawa, "Development of Aromatic Polymer Electrolyte Membrane with High Conductivity and Durability for Fuel Cell," *Polymer Journal*, vol. 41 (2), pp. 95–104, 2009.

[44] V. Stanic and M. Hoberecht, "Mechanism of pinhole formation in membrane electrode assemblies for PEM fuel cells," *NASA Technical Reports*, 2004.

[45] X. Huang, R. Solasi, Y. Zou, M. Feshler, K. Reisnider, D. Condit, S. Burlatsky, and T. Madden, "Mechanical Endurance of Polymer Electrolyte Membrane and PEM Fuel Cell Durability," *Journal of Polymer Science Part B - Polymer Physics*, vol. 44, pp. 2346–2357, 2006.

[46] M. N. Tsampas, A. Pikos, S. Brosda, A. Katsaounis, and C. Vayenas, "The Effect of Membrane Thickness on the Conductivity of Nafion," *Electrochimica Acta*, vol. 51, pp. 2743–2755, 2006.

[47] A. Kusoglu, A. Karlsson, M. Santare, S. Cleghorn, and W. Johnson, "Mechanical Response of Fuel Cell Membranes Subjected to a Hygro-Thermal Cycle," *Journal of Power Sources*, vol. 161, pp. 987–996, 2006.

[48] M. Cappadonia, J. Erning, U. Stimming, and S. Niaki, "Conductance of Nafion 117 membranes as a function of temperature and water content," *Solid State Ionics*, vol. 77, pp. 65–69, 1995.

[49] M. Oszcipok, D. Riemann, U. Kronenwett, M. Kreideweis, and M. Zedda, "Statistic analysis of operational influences on the cold start behaviour of PEM fuel cells," *Journal of Power Sources*, vol. 145, pp. 407–415, 2005.

[50] A. Pesaran, G.-H. Kim, and J. Gonder, "PEM Fuel Cell Freeze and Rapid Startup Investigation," *NREL/MP*, vol. 1, p. 8760, 2005.

[51] A. LaConti, C. Mittelsteadt, and R. McDonald, "Polymer Electrolyte Membrane Degradation Mechanisms in Fuel Cells - Findings Over the Past 30 Years and Comparison with Electrolyzers," *ECS Transactions*, vol. 1, pp. 199–219, 2006.

[52] A. Bonakdarpour, T. Dahn, R. Atanasoski, M. Debe, and J. Dahn, "H_2O_2 Release During Oxygen Reduction Reaction on Pt Nanoparticles," *Electrochemical and Solid-State Letters*, vol. 11, pp. B208–B211, 2008.

[53] A. Schneider, L. Colmenares, Y. Seidel, Z. Jusys, B. Wickman, B. K. B, and R. Behm, "Transport effects in the oxygen reduction reaction on nanostructured, planar glassy carbon supported Pt/GC model electrodes," *Physical Chemistry Chemical Physics*, vol. 10, pp. 1931–1943, 2008.

[54] Y. Seidel, A. Schneider, Z. Jusys, B. Wickman, B. Kasemo, and R. Behm, "Mesoscopic mass transport effects in electrocatalytic processes," *Faraday Discussions*, vol. 140, pp. 167–184, 2008.

[55] G. Pourcelly, A. Oikonomou, C. Gavach, and H. Hurwitz, "Influence of the water content on the kinetics of counter-ion transport in perfluorosulphonic membranes," *Journal of Electroanalytical Chemistry*, vol. 287, pp. 43–59, 1990.

[56] A. Pozio, R. Silva, M. Francesco, and M. D. G. L, "Nafion degradation in PEFCs from end plate iron contamination," *Electrochimica Acta*, vol. 48, pp. 1543–1549, 2003.

[57] D. Ludlow, C. Calebrese, S. Yu, C. Dannehy, D. Jacobson, D. Hussey, M. Arif, M. Jensen, and G. Eisman, "PEM fuel cell membrane hydration measurement by neutron imaging," *Journal of Power Sources*, vol. 162, pp. 271–278, 2006.

[58] W. Yan, S. Mei, C. Soong, Z. Liu, and D. Song, "Experimental study on the performance of PEM fuel cells with interdigitated flow channels," *Journal of Power Sources*, vol. 160, pp. 116–122, 2006.

[59] A. Taniguchi, T. Akita, K. Yasuda, and Y. Miyazaki, "Analysis of electrocatalyst degradation in PEMFC caused by cell reversal during fuel starvation," *Journal of Power Sources*, vol. 130, pp. 42–49, 2004.

[60] H. Ju and C. Wang, "Experimental Validation of a PEM Fuel Cell Model by Current Distribution Data," *Journal of Electrochemical Society*, vol. 151, pp. A1954–A1960, 2004.

[61] C. Reiser, L. Bregoli, T. Patterson, J. Yi, J. Yang, M. Perry, and T. Jarvi, "A Reverse-Current Decay Mechanism for Fuel Cells," *Electrochemical Solid-State Letters*, vol. 8, pp. A273–A276, 2005.

[62] J. Wu, X. Yuan, J. Martin, H. Wang, J. Zhang, J. Shen, S. Wu, and W. Merida, "A review of PEM fuel cell durability Degradation mechanisms and mitigation strategies," *Journal of Power Sources*, vol. 184, pp. 104–119, 2008.

[63] M. Schulze, A. Schneider, and E. Gülzow, "Alteration of the distribution of the platinum catalyst in membrane-electrode assemblies during PEMFC operation," *Journal of Power Sources*, vol. 127, pp. 213–221, 2004.

[64] Y. Shao-Horn, W. Sheng, S. Chen, P. Ferreira, E. Holby, and D. Morgan, "Instability of Supported Platinum Nanoparticles in Low-Temperature Fuel Cells," *Topics in Catalysis*, vol. 46, pp. 285–305, 2007.

[65] W. Bi, G. Gray, and T. Fuller, "PEM Fuel Cell Pt/C Dissolution and Deposition in Nafion Electrolyte," *Electrochemical and Solid-State Letters*, vol. 46, pp. 287–305, 2007.

[66] V. Atrazhev, S. Burlatsky, N. Cipollini, D. Condit, and N. Erikhman, "Aspects of PEMFC Degradation," *ECS Transactions*, vol. 1, pp. 239–246, 2006.

[67] K. Yasuda, A. Taniguchi, T. Akita, T. Ioroi, and Z. Siroma, "Platinum dissolution and deposition in the polymer electrolyte membrane of a PEM fuel cell as studied by potential cycling," *Physical Chemistry Chemical Physics*, vol. 8, pp. 746–752, 2006.

[68] M. Pourbaix, *Atlas of electrochemical equilibria in aqueous solutions.* N A C E International, 1966.

[69] G. Liu, H. Zhang, H. Zhong, J. Hu, D. Xu, and Z. Shao, "A novel sintering resistant and corrosion resistant Pt_4ZrO_2/C catalyst for high temperature PEMFCs," *Electrochimica Acta*, vol. 51, pp. 5710–5714, 2006.

[70] T. Ioroi, H. S. ans S. Yamazaki, Z. Siroma, N. Fujiwara, and K. Yasuda, "Stability of Corrosion-Resistant Magneli-Phase Ti_4O_7-Supported PEMFC Catalysts at High Potentials," *Journal of The Electrochemical Society*, vol. 155, pp. B321–B326, 2008.

[71] S. Ball, B. Theobald, D. Thompsett, and S. Hudson, "Enhanced Stability of PtCo catalysts for PEMFC," *ECS Transactions*, vol. 1, pp. 141–152, 2008.

[72] T. Frelink, W. Visscher, and J. van Veen, "On the role of Ru and Sn as promotors of methanol electro-oxidation over Pt," *Surface Science*, pp. 353–360, 1995.

[73] X. Cheng, L. Chen, C. Peng, Z. Chen, Y. Zhang, and Q. Fan, "Catalyst Microstructure Examination of PEMFC Membrane Electrode Assemblies vs Time," *Journal of The Electrochemical Society*, vol. 151, pp. A48–A52, 2004.

[74] K. More, J. Bentley, and K. Reeves, "Microstructural Characterization Of PEM Fuel Cell MEAs." `http://www.hydrogen.energy.gov/pdfs/review06/fc_27_more.pdf`. Last accessed 2014-03-02.

[75] M. Schulze, N. Wagner, T. Kaz, and K. Friedrich, "Combined electrochemical and surface analysis investigation of degradation processes in polymer electrolyte membrane fuel cells," *Electrochimica Acta*, vol. 52, pp. 2328–2336, 2007.

[76] S. Gottesfeld and J. Pafford, "A New Approach to the Problem of Carbon Monoxide Poisoning in Fuel Cells Operating at Low Temperatures," *Journal of Electrochemical Society*, vol. 49, pp. 2651–2652, 1988.

[77] C. Sishtla, G. Koncar, R. Platon, S. Gamburzev, A. Appleby, and O. Velev, "Performance and enducance of a PEMFC operated with synthetic reformate fuel feed," *Journal of Power Sources*, vol. 71, pp. 249–255, 1998.

[78] T. Isono, S. Suzuki, M. Kaneko, Y. Akiyama, Y. Miyake, and I. Yonezu, "Development of a high-performance PEFC module operated by reformed gas," *Journal of Power Sources*, vol. 86, pp. 269–273, 2000.

[79] S. Alayoglu, A. Nilekar, M. Mavrikakis, and B. Eichhorn, "Ru/Pt core-shell nanoparticles for preferential oxidation of carbon monoxide in hydrogen," *Nature Materials*, vol. 7, pp. 333–338, 2008.

[80] T. Tingelöf, L. Hedström, N. Holmström, P. Alvfors, and G. Lindbergh, "The influence of CO_2, CO and air bleed on the current distribution of a polymer electrolyte fuel cell International," *Journal of Hydrogen Energy*, vol. 33, pp. 2064–2072, 2008.

[81] H. Tang, Z. Ramani, M. Qiand, and J. Elter, "PEM fuel cell cathode carbon corrosion due to the formation of airfuel boundary at the anode," *Journal of Power Sources*, vol. 158, pp. 1306–1312, 2006.

[82] D. Harris and M. Bertolucci, *Symmetry and Spectroscopy - An Introduction to Vibrational and Electronic Spectroscopy*. Dover Publications, Inc, New York, 1978.

[83] A. Gruger, A. Regis, T. Schmatko, and P. Colomban, "Nanostructure of Nafion membranes at different states of hydration: An IR and Raman study," *Vibrational Spectroscopy*, vol. 26, pp. 215–225, 2001.

[84] M. Holber, A. Haug, M. Schulze, A. Selimovic, S. Escribano, L. Guetaz, L. Merlo, K. A. Friedrich, P. Jacobsson, and P. Johansson, "Spectroscopic Detection of Local Platinum Degradation in Polymer Electrolyte Membrane Fuel Cells," *Submitted*, 2014.

[85] M. Minsky, "Memoir on Inventing the Confocal Scanning Microscope," *Scanning*, vol. 10, pp. 128–138, 1988.

[86] J. Zhang, *PEM Fuel Cell Electrocatalysts and Catalyst Layers: Fundamentals and Applications*. Springer, 2008.

[87] R. Toyoshima, M. Shimura, M. Yoshida, Y. Monya, K. Suzuki, K. Amemiya, K. Mase, B. S. Mun, and H. Kondoh, "A near-ambient-pressure XPS study on catalytic CO oxidation reaction over a Ru(1010) surface," *Surface Science*, vol. 621, pp. 128–132, 2014.

[88] L. Guetaz, S. Escribano, and O. Sicardy, "Study by electron microscopy of proton exchange membrane fuel cell membrane-electrode assembly degradation mechanisms: Influence of local conditions," *Journal of Power Sources*, vol. 212, pp. 169–178, 2012.